Table 3 Histology and immunohistochemistry results

	Clear cell RCC	Other subtypes	p Value
Number of tumours	90	32	
MVD (CD31)	219 (226.4±87.3)	98.5 (110.3±80.6)	<0.0001*
VASH1	76 (85.9±72.5)	15 (25.5±30.9)	<0.0001*
VEGFR2	8.5 (16.7±23.2)	0 (1.84±2.64)	<0.0001*
VEGF			
Membranous or mixed	62	9	0.0001*
Cytoplasmic	28	23	
VASH1/CD31	0.342 (0.372±0.270)	0.172 (0.235±0.210)	0.0079*
VEGFR2/CD31	0.045 (0.0710±0.0924)	0 (0.0176±0.0260)	<0.0001*

*p<0.05.
MVD, microvessel density; RCC, renal cell carcinoma; VASH1, vasohibin-1; VEGF, vascular endothelial growth factor; VEGFR2, vascular endothelial growth factor receptor type 2.

to pT factor (p=0.0253), pN factor (p=0.0075), distant metastasis (p<0.0001) and TNM stage (p<0.0001). Overall survival was not significantly related to age (p=0.1597), histology (p=0.8587), Fuhrman's nuclear grading (p=0.1482), MVD (p=0.7859), expression of VASH1 (p=0.4720) or VEGFR2 (p=0.8854; figure 3).

Clinical follow-up information was available for 87 cases of curatively operated tumours not accompanied by distant metastasis at the time of the operation. Sixteen of 62 tumours (25.8%) with low VASH1 expression recurred compared with only 2 of 25 tumours (8.0%) with high VASH1 expression. VASH1 expression was significantly associated with disease-free survival (p=0.030). pT factor and TNM stage were also significant prognostic factors (p=0.0012 and p = 0.0018, respectively). pN factor, age, tumour histology, Fuhrman's nuclear grading, MVD and VEGFR2 did not have significant prognostic

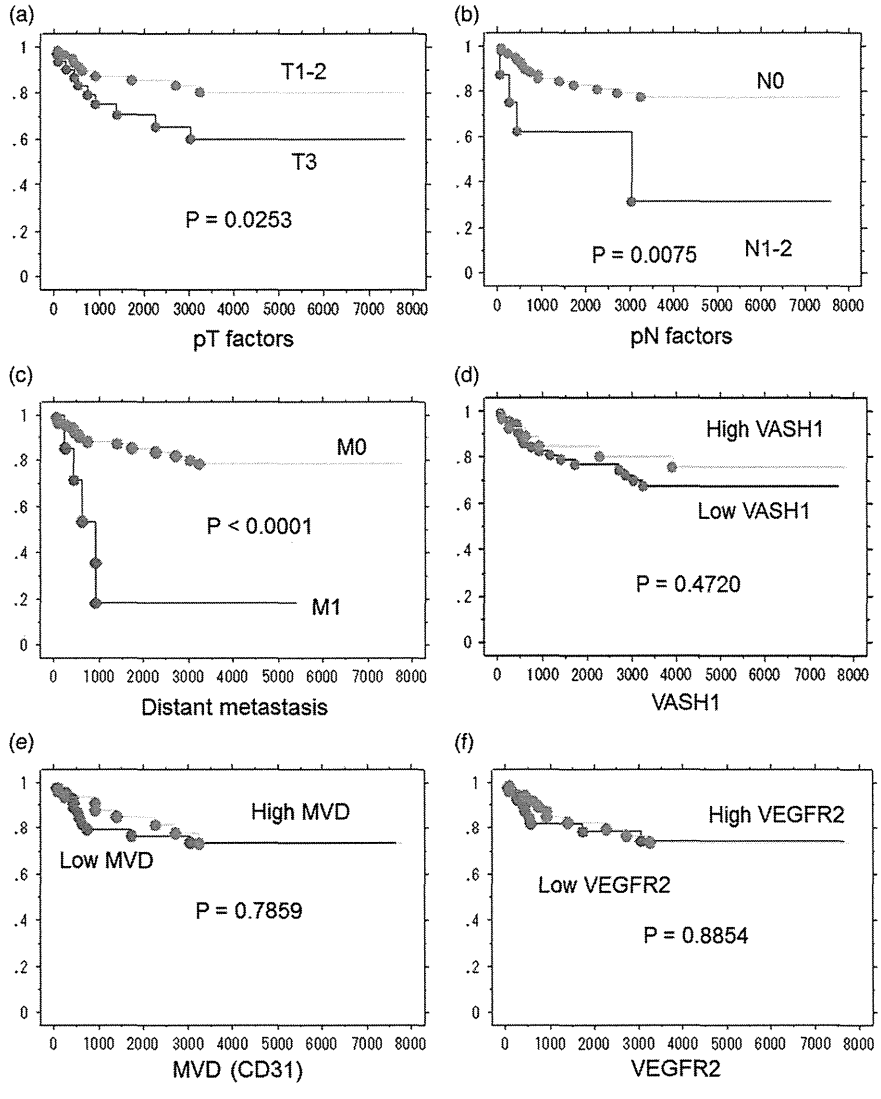

Figure 3 Kaplan–Meier analyses of overall survival according to pT factor (A), pN factor (B), distant metastasis (C), vasohibin-1 (VASH1) expression (D), microvessel density (MVD) (E) and vascular endothelial growth factor receptor type 2 (VEGFR2) expression (F).

correlation (p=0.0586, p = 0.3987, p = 0.9466, p = 0.4274, p = 0.4540 and p = 0.3280, respectively; figure 4). The Cox model of multivariable disease-free survival that included VASH1 (at the cut-off level of 95 per field), pT factor and stage indicated that VASH1 and stage were independent prognostic factors (p=0.019; HR 0.486, and p=0.024; HR 4.053; table 4).

DISCUSSION

VASH1 is an endothelium-derived negative feedback regulator of angiogenesis.[20] Two isoforms of human VASH1 are known: full-length VASH1A and its splicing variant, VASH1B. Human VASH1A protein is composed of 365 amino acid residues and human VASH1B protein is composed of 204 amino acid residues. Both forms of VASH have anti-angiogenic activity.[27]

VASH1 correlates positively with tumour grade of endometrial cancer.[24] Its expression is higher in uterine cervical cancer tissue than in normal uterine cervical tissue.[25] In breast cancers, VASH1 expression correlates with VEGF, bFGF and VEGFR2,[23] and high VASH1 expression indicates a poor prognosis for breast cancer.[23] Miyazaki *et al*[26] reported recently that VASH1 is an independent prognostic factor of upper urinary tract urothelial carcinoma. The expression of VASH1 in renal cell carcinoma has not been well studied with only one report being available for VASH1 expression in renal cell carcinoma.[28] The expression level of VASH1 in renal cell carcinoma tissue was significantly lower than that in non-tumorous renal tissues. The possible prognostic impact of VASH1 has not been investigated. The aim of this study was to elucidate VASH1 expression and to identify possible relationships between VASH1 expression and various clinicopathological factors including the prognosis for renal cell carcinoma.

We found that high VASH1 expression correlated with better disease-free survival of curatively operated patients with renal cell carcinoma whereas MVD did not correlate with disease-free survival or overall survival. The significance of MVD on the prognosis of kidney cancer is controversial. High MVD has been reported to be an indicator of better prognosis,[29–36] worse prognosis,[12 37–39] or to have no prognostic value.[40 41] It is interesting that only VASH1 expression had prognostic significance in our study, although VASH1 and MVD correlated positively. Renal cell carcinomas seem to have some different mechanisms of VASH1-related angiogenetic feedback mechanism. Renal tumours where the vessels are less covered by VASH1 seem to have aggressive behaviour and tumours with an abnormal/broken VASH1-related vascular mechanism are likely to be aggressive.

Our series included three patients who died of other diseases (pneumonia, liver cirrhosis and sepsis). This might account for the finding that VASH1 was associated with disease-free survival but was not associated with overall survival.

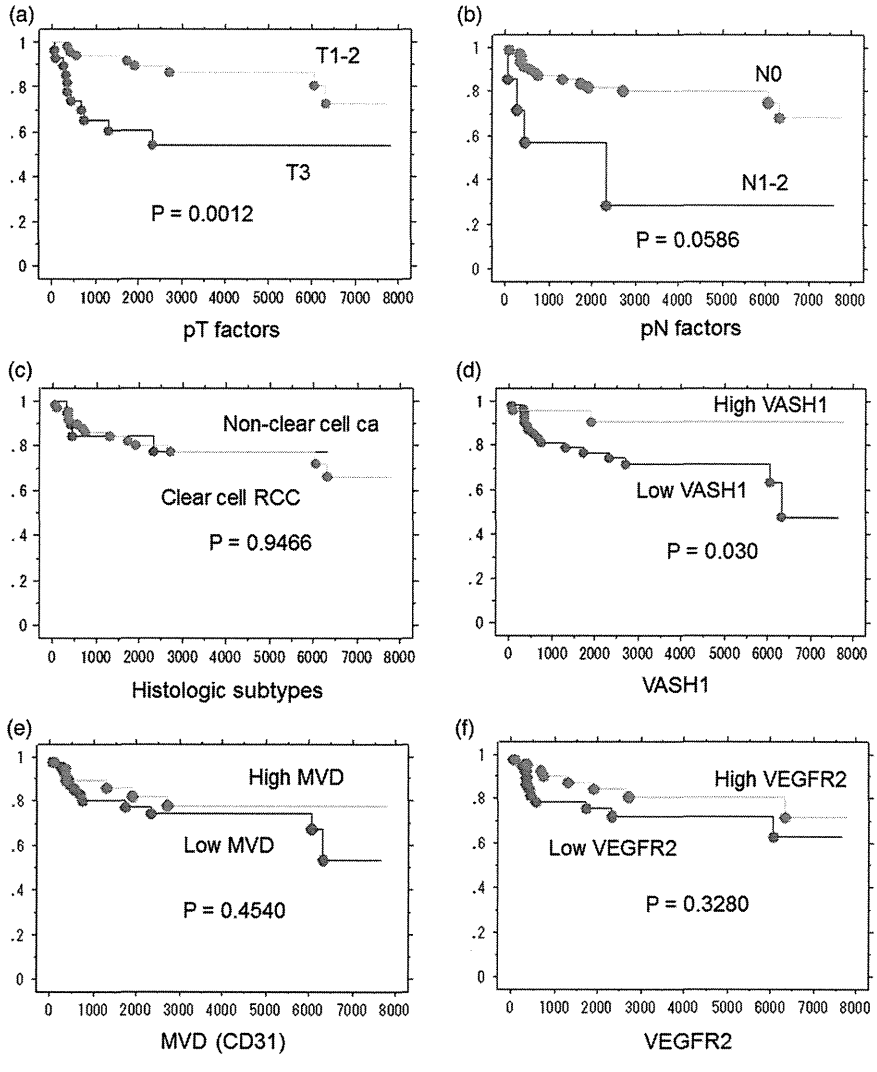

Figure 4 Kaplan–Meier analyses of disease-free survival according to pT factor (A), pN factor (B), histology (C), vasohibin-1 (VASH1) expression (D), microvessel density (MVD) (E) and vascular endothelial growth factor receptor type 2 (VEGFR2) expression (F).

Table 4 Cox proportional hazards model for cancer-specific survival

		Univariate		Multivariable	
Parameter	Criteria	p Value	HR (95% CI)	p Value	HR (95% CI)
pT	1/2 vs 3	0.0028*	4.168 (1.636 to 10.620)	0.065	3.420 (0.927 to 12.609)
pN	0 vs ½	0.0729	3.122 (0.899 to 10.839)		
pStage	1/2 vs ¾	0.0038*	3.992 (1.563 to 10.194)	0.024*	4.035 (1.197 to 13.600)
Histology	Clear cell vs others	0.9466	0.963 (0.315 to 2.940)		
Fuhrman's grade	1/2 vs ¾	0.4312	0.640 (0.210 to 1.946)		
MVD	<177 vs ≥177	0.4564	0.697 (0.269 to 1.805)		
VASH1	<95 vs ≥95	0.0461*	0.218 (0.049 to 0.974)	0.019*	0.486 (0.280 to 0.890)
VASH1	(continuum)	0.2815	0.996 (0.988 to 1.004)		
VEGFR2	<6 vs ≥6	0.3322	0.630 (0.247 to 1.605)		

* p<0.05.
MVD, microvessel density; VASH1, vasohibin-1; VEGF, vascular endothelial growth factor; VEGFR2, vascular endothelial growth factor receptor type 2.

We found that the VASH1 density histogram was bimodal, although there was an overlap (figure 2). The VASH1 density histogram of clear cell carcinoma was also bimodal (data not shown). According to Brannon and coworkers, unsupervised consensus clustering of DNA microarray can divide clear cell carcinoma into two categories.[42] Clear cell carcinomas designated type A (ccA) have markedly improved disease-specific survival compared with type B (ccB) tumours. The pathway analysis of the angiogenesis gene set showed that ccA and ccB are highly dissimilar. VASH1 expression might differ between ccA and ccB.

We showed that high levels of VASH1 expression were associated with a good prognosis for renal cell carcinoma but, in breast cancer, a high level of VASH1 expression was associated with a poor prognosis.[23] Almost all the vessels in renal cell carcinoma are sandwiched by the tumour cells without any interventional tissue. However, in breast cancers the 'tumour vessels' do not always touch the tumour cells as desmoplastic stromal cells are usually present between the vessels and the breast tumour cells. Renal cell carcinoma typically shows apparent hypervascularity by angiographic study while breast cancer shows lower vascularity. These differences might be important for the VASH1-related vascular mechanism and the different impact of VASH1 on the prognosis of kidney cancer and breast cancer.

We also found that VASH1 expression was significantly lower in tumours with fat invasion than in those without fat invasion. Lower VASH1 expression by itself or an imbalance between VASH1 level and the levels of other angiogenic/anti-angiogenic factors might influence fat invasion in renal cell carcinoma. VASH1 may play an important role in the cancer–stroma interaction in the cancer microenvironment. Cancer-associated stromal cells are important for cancer invasion, especially through their production of matrix metalloproteinases.[43] VASH1 is produced in the bone marrow,[44] and bone marrow-derived myofibroblasts have been reported to contribute to the cancer-induced stromal reaction.[45] The relationship between VASH1 and cancer-associated stromal fibroblast-type cells is an attractive topic for further investigation.

We identified VASH1 expression in the endothelium of the kidney cancer blood vessels. VASH1 was higher in clear cell carcinoma than other subtypes such as MVD and VEGFR2. The VEGF expression pattern differed between clear cell carcinoma and non-clear cell carcinoma. Sandlund *et al*[32] reported that MVD is higher in clear cell renal cell carcinoma than in papillary renal cell carcinoma. These results suggest that the angiogenic mechanism differs between clear cell carcinoma and non-clear cell carcinoma. Clear cell renal cell carcinoma is known to overexpress VEGF and HIF-1 because of von Hippel-Lindau gene dysfunction,[3–6] whereas other subtypes of renal cell carcinoma do not have this abnormality. The tumour histology might be important to choose anti-angiogenic therapy.

VASH1 is naturally present in the human body and the administration of VASH1 to patients seems to be possible. VASH1 might be able to control the local invasion or distant metastasis of renal cell carcinoma. VASH1 has a different anti-angiogenic mechanism from that of sorafenib, sunitinib and bevacizumab. Combined therapy with these agents may also be promising. The development of VASH1 therapy for renal cell carcinoma through in vivo models, for example, is encouraged.

Take-home messages

- Microvessel density, vasohibin-1 (VASH1) and vascular endothelial growth factor receptor type 2 (VEGFR2) expression were significantly higher in clear cell renal carcinoma than in other subtypes.
- The pattern of VEGF expression differed significantly between clear cell renal carcinoma and other histological subtypes.
- VASH1 was significantly associated with disease-free survival in curatively operated patients with renal cell carcinoma.

Acknowledgements We thank Kumiko Ikoma and Yoshiko Murakawa for their technical assistance and Hiroko Murakami for her secretarial assistance.

Contributors All the authors participated directly in the planning, execution and analysis of the study.

Funding This study was supported by Kawasaki Medical School Research Project (#21-106).

Competing interests None.

Patient consent Obtained.

Ethics approval This study received ethics approval from the Institutional Review Board of Kawasaki Medical School (approval no 372).

REFERENCES

1 Lang EK. Arteriographic assessment and staging of renal-cell carcinoma. Analysis of a series of 120 patients. *Radiology* 1971;101:17–27.
2 Mattern J, Volm M. Microvessel density and vascular endothelial growth factor expression in human tumors of different localization. *Oncol Rep* 1996;3:465–8.
3 Kondo K, Kaelin WG Jr. The von Hippel-Lindau tumor suppressor gene. *Exp Cell Res* 2001;264:117–25.
4 Brown LF, Berse B, Tognazzi K, *et al*. Vascular permeability factor mRNA and protein expression in human kidney. *Kidney Int* 1992;42:1457–61.
5 Takahashi A, Sasaki H, Kim SJ, *et al*. Markedly increased amounts of messenger RNAs for vascular endothelial growth factor and placenta growth factor in renal cell carcinoma associated with angiogenesis. *Cancer Res* 1994;54:4233–7.
6 Nicol D, Hii SI, Walsh M, *et al*. Vascular endothelial growth factor expression is increased in renal cell carcinoma. *J Urol* 1997;157:1482–6.
7 Chang SG, Jeon SH, Lee SJ, *et al*. Clinical significance of urinary vascular endothelial growth factor and microvessel density in patients with renal cell carcinoma. *Urology* 2001;58:904–8.
8 Hemmerlein B, Kugler A, Ozisik R, *et al*. Vascular endothelial growth factor expression, angiogenesis, and necrosis in renal cell carcinomas. *Virchows Arch* 2001;439:645–52.
9 Minardi D, Lucarini G, Filosa A, *et al*. Prognostic role of tumor necrosis, microvessel density, vascular endothelial growth factor and hypoxia inducible factor-1alpha in patients with clear cell renal carcinoma after radical nephrectomy in a long term follow-up. *Int J Immunopathol Pharmacol* 2008;21:447–55.
10 Verheul HM, van Erp K, Homs MY, *et al*. The relationship of vascular endothelial growth factor and coagulation factor (fibrin and fibrinogen) expression in clear cell renal cell carcinoma. *Urology* 2010;75:608–14.
11 Slaton JW, Inoue K, Perrotte P, *et al*. Expression levels of genes that regulate metastasis and angiogenesis correlate with advanced pathological stage of renal cell carcinoma. *Am J Pathol* 2001;158:735–43.
12 Fukata S, Inoue K, Kamada M, *et al*. Levels of angiogenesis and expression of angiogenesis-related genes are prognostic for organ-specific metastasis of renal cell carcinoma. *Cancer* 2005;103:931–42.
13 Kawata N, Yagasaki H, Yuge H, *et al*. Histopathologic analysis of angiogenic factors in localized renal cell carcinoma: the influence of neoadjuvant treatment. *Int J Urol* 2001;8:275–81.
14 Suzuki K, Morita T, Hashimoto S, *et al*. Thymidine phosphorylase/platelet-derived endothelial cell growth factor (PD-ECGF) associated with prognosis in renal cell carcinoma. *Urol Res* 2001;29:7–12.
15 Tawfik OW, Kramer B, Shideler B, *et al*. Prognostic significance of CD44, platelet-derived growth factor receptor alpha, and cyclooxygenase 2 expression in renal cell carcinoma. *Arch Pathol Lab Med* 2007;131:261–7.
16 Xu L, Tong R, Cochran DM, *et al*. Blocking platelet-derived growth factor-D/ platelet-derived growth factor receptor beta signaling inhibits human renal cell carcinoma progression in an orthotopic mouse model. *Cancer Res* 2005;65:5711–19.
17 Sulzbacher I, Birner P, Traxler M, *et al*. Expression of platelet-derived growth factor-alpha alpha receptor is associated with tumor progression in clear cell renal cell carcinoma. *Am J Clin Pathol* 2003;120:107–12.
18 Izutsu T, Konda R, Sugimura J, *et al*. Brain-specific angiogenesis inhibitor 1 is a putative factor for inhibition of neovascular formation in renal cell carcinoma. *J Urol* 2011;185:2353–8.
19 Baltaci S, Orhan D, Gogus C, *et al*. Thrombospondin-1, vascular endothelial growth factor expression and microvessel density in renal cell carcinoma and their relationship with multifocality. *Eur Urol* 2003;44:76–81.
20 Watanabe K, Hasegawa Y, Yamashita H, *et al*. Vasohibin as an endothelium-derived negative feedback regulator of angiogenesis. *J Clin Invest* 2004;114:898–907.
21 Sato Y, Sonoda H. The vasohibin family: a negative regulatory system of angiogenesis genetically programmed in endothelial cells. *Arterioscler Thromb Vasc Biol* 2007;27:37–41.
22 Tamaki K, Sasano H, Maruo Y, *et al*. Vasohibin-1 as a potential predictor of aggressive behavior of ductal carcinoma in situ of the breast. *Cancer Sci* 2010;101:1051–8.
23 Tamaki K, Moriya T, Sato Y, *et al*. Vasohibin-1 in human breast carcinoma: a potential negative feedback regulator of angiogenesis. *Cancer Sci* 2009;100:88–94.
24 Yoshinaga K, Ito K, Moriya T, *et al*. Expression of vasohibin as a novel endothelium-derived angiogenesis inhibitor in endometrial cancer. *Cancer Sci* 2008;99:914–19.
25 Yoshinaga K, Ito K, Moriya T, *et al*. Roles of intrinsic angiogenesis inhibitor, vasohibin, in cervical carcinomas. *Cancer Sci* 2011;102:446–51.
26 Miyazaki Y, Kosaka T, Mikami S, *et al*. The prognostic significance of vasohibin-1 expression in patients with upper urinary tract urothelial carcinoma. *Clin Cancer Res* 2012;18:4145–53.
27 Sato Y. The vasohibin family: novel regulators of angiogenesis. *Vascul Pharmacol* 2012;56:262–6.
28 Zhao G, Yang Y, Tang Y, *et al*. Reduced expression of vasohibin-1 is associated with clinicopathological features in renal cell carcinoma. *Med Oncol* 2012;29:3325–34.
29 Rioux-Leclercq N, Epstein JI, Bansard JY, *et al*. Clinical significance of cell proliferation, microvessel density, and CD44 adhesion molecule expression in renal cell carcinoma. *Hum Pathol* 2001;32:1209–15.
30 Schraml P, Struckmann K, Hatz F, *et al*. VHL mutations and their correlation with tumour cell proliferation, microvessel density, and patient prognosis in clear cell renal cell carcinoma. *J Pathol* 2002;196:186–93.
31 Yildiz E, Ayan S, Goze F, *et al*. Relation of microvessel density with microvascular invasion, metastasis and prognosis in renal cell carcinoma. *BJU Int* 2008;101:758–64.
32 Sandlund J, Hedberg Y, Bergh A, *et al*. Evaluation of CD31 (PECAM-1) expression using tissue microarray in patients with renal cell carcinoma. *Tumour Biol* 2007;28:158–64.
33 Sabo E, Boltenko A, Sova Y, *et al*. Microscopic analysis and significance of vascular architectural complexity in renal cell carcinoma. *Clin Cancer Res* 2001;7:533–7.
34 Toge H, Inagaki T, Kojimoto Y, *et al*. Angiogenesis in renal cell carcinoma: the role of tumor-associated macrophages. *Int J Urol* 2009;16:801–7.
35 Mertz KD, Demichelis F, Kim R, *et al*. Automated immunofluorescence analysis defines microvessel area as a prognostic parameter in clear cell renal cell cancer. *Hum Pathol* 2007;38:1454–62.
36 Imao T, Egawa M, Takashima H, *et al*. Inverse correlation of microvessel density with metastasis and prognosis in renal cell carcinoma. *Int J Urol* 2004;11:948–53
37 Yoshino S, Kato M, Okada K. Prognostic significance of microvessel count in low stage renal cell carcinoma. *Int J Urol* 1995;2:156–60.
38 Joo HJ, Oh DK, Kim YS, *et al*. Increased expression of caveolin-1 and microvessel density correlates with metastasis and poor prognosis in clear cell renal cell carcinoma. *BJU Int* 2004;93:291–6.
39 Miyata Y, Koga S, Kanda S, *et al*. Expression of cyclooxygenase-2 in renal cell carcinoma: correlation with tumor cell proliferation, apoptosis, angiogenesis, expression of matrix metalloproteinase-2, and survival. *Clin Cancer Res* 2003;9:1741–9.
40 MacLennan GT, Bostwick DG. Microvessel density in renal cell carcinoma: lack of prognostic significance. *Urology* 1995;46:27–30.
41 Minardi D, Lucarini G, Mazzucchelli R, *et al*. Prognostic role of Fuhrman grade and vascular endothelial growth factor in pT1a clear cell carcinoma in partial nephrectomy specimens. *J Urol* 2005;174:1208–12.
42 Brannon AR, Reddy A, Seiler M, *et al*. Molecular stratification of clear cell renal cell carcinoma by consensus clustering reveals distinct subtypes and survival patterns. *Genes Cancer* 2010;1:152–63.
43 Kanomata N, Nakahara R, Oda T, *et al*. Expression and localization of mRNAs for matrix metalloproteinases and their inhibitors in mixed bronchioloalveolar carcinomas with invasive components. *Mod Pathol* 2005;18:828–37.
44 Kimura H, Miyashita H, Suzuki Y, *et al*. Distinctive localization and opposed roles of vasohibin-1 and vasohibin-2 in the regulation of angiogenesis. *Blood* 2009;113:4810–18.
45 Ishii G, Sangai T, Oda T, *et al*. Bone-marrow-derived myofibroblasts contribute to the cancer-induced stromal reaction. *Biochem Biophys Res Commun* 2003;309:232–40.

FULL PAPER

BJC

British Journal of Cancer (2013), 1–7 | doi: 10.1038/bjc.2013.169

Keywords: vasohibin-1; prostate cancer; angiogenesis

The prognostic significance of vasohibin-1 expression in patients with prostate cancer

T Kosaka[1,4], Y Miyazaki[1,4], A Miyajima[1], S Mikami[2], Y Hayashi[2], N Tanaka[1], H Nagata[1], E Kikuchi[1], K Nakagawa[1], Y Okada[2], Y Sato[3] and M Oya[1]

[1]*Department of Urology, Keio University School of Medicine, 35 Shinanomachi, Shinjuku-ku, Tokyo 160-8582, Japan;* [2]*Department of Pathology, Keio University School of Medicine, 35 Shinanomachi, Shinjuku-ku, Tokyo 160-8582, Japan and* [3]*Department of Vascular Biology, Institute of Development, Aging, and Cancer, Tohoku University, 4-1, Seiryo-machi, Aoba-ku, Sendai 980-9575, Japan*

Background: We recently isolated vasohibin-1 (VASH1), a novel angiogenic molecule that is specifically expressed in activated vascular endothelial cells (ECs), and the status of VASH1 expression has been documented in various cancer angiogenesis. The aim of this study was to assess the prognostic value of VASH1 expression in prostate cancer (PCa).

Methods: In this study, we retrospectively analysed the clinical records and evaluated the VASH1 expression of tumour microvessels in 167 patients with PCa who underwent radical prostatectomy. We immunohistochemically examined the microvessels positive for anti-CD34 as microvessel density (MVD) and the microvessels with activated ECs positive for VASH1 density.

Results: We found that the VASH1 expression was restricted to ECs in the tumour stroma. VASH1 density was significantly associated with pathological T stage, Gleason score and MVD. The 5-year PSA recurrence-free survival rate was 58.8% in patients with higher VASH1 density (≧12 per mm^2) and 89.1% in patients with lower VASH1 density (<12 per mm^2), respectively ($P<0.001$). Microvessel density was not an independent predictor of PSA recurrence. Multivariate analysis revealed that high VASH1 density was an independent prognostic indicator of PSA recurrence ($P=0.007$, HR = 2.950).

Conclusion: VASH1 density represents a clinically relevant predictor of patient prognosis and can be a new biomarker that would provide additional prognostic information in PCa.

Prostate cancer (PCa) is one of the most commonly diagnosed malignant tumours in men and the second leading cause of cancer-related deaths in the United States (Jemal *et al*, 2010). Nowadays, there are still few effective therapeutic options for advanced PCa (Scher and Sawyers, 2005; Chen *et al*, 2008). One of the most troublesome aspects of PCa is that androgen-dependent PCa inevitably progresses to highly aggressive and life-threatening castration-resistant prostate cancer after androgen ablation therapy. The key molecular events associated with PCa progression remains to be elucidated.

Angiogenesis, which is the formation of new blood vessel networks, not only plays a role in human normal development but also in pathophysiological conditions such as inflammation and cancer (Folkman, 1971; Sato, 2003). The development and establishment of blood supply has an important role in the development and growth of cancer cells by providing oxygen, nutrients and growth factors. In addition to its traditional role, angiogenesis is one of the potential pathways that contribute to solid tumour progression and metastasis by allowing cancer cells direct access to vessels. In general, angiogenesis is regulated by a balance between stimulatory and inhibitory factors (Sato and Sonoda, 2007, Sato, 2012). Molecules such as CD34, von Willebrand factor and vascular endothelial-cadherin, which are specifically expressed in vascular endothelial cells (ECs), could serve as biomarkers of angiogenesis (Weidner *et al*, 1991). One of the parameters of angiogenesis in neoplasms is microvessel density

*Correspondence: Dr T Kosaka; E-mail: takemduro@gmail.com
[4]These authors contributed equally to this work.

Received 7 February 2013; revised 21 March 2013; accepted 28 March 2013

(MVD). In PCa, several studies indicated that MVD served as a predictor of poorly differentiated tumours and biochemical failure after treatment (Weidner *et al*, 1993; Bettencourt *et al*, 1998; Borre *et al*, 1998; Rubin *et al*, 1999; Krupski *et al*, 2000; Josefsson *et al*, 2005; Concato *et al*, 2007, 2009; Kosaka *et al*, 2007). However, to date the prognostic role of MVD in PCa has not been fully characterised. This is because those angiogenic molecules are expressed in quiescent ECs as well as in activated ECs, and thus cannot reflect 'angiogenic activity' alone.

We recently isolated vasohibin-1 (VASH1), a novel angiogenic molecule, that is specifically expressed in ECs and upregulated by vascular endothelial growth factor (VEGF) and fibroblast growth factor 2 (FGF-2) (Watanabe *et al*, 2004; Kimura *et al*, 2009). Previous studies found that the expression of VASH1 was restricted to ECs of blood vessels in the tumour stroma and correlated with the expression of VEGF and FGF-2 in tumour cells (Hosaka *et al*, 2009). No one has ever characterised the expression of VASH1 in relation to tumour angiogenesis in PCa. In this study, we will evaluate whether the expression of VASH1 can serve as a more accurate biomarker of tumour angiogenesis compared with MVD.

We will examine the expression of VASH1 and MVD in PCa specimens acquired by primary surgery and investigate whether VASH1 expression reflects angiogenic activity in PCa and if this is related to the clinical outcome.

MATERIALS AND METHODS

Patients selection. Samples of archival paraffin-embedded tissue sections and clinicopathological features were obtained from 167 patients with PCa diagnosed and operated on at Keio University hospital. One hundred and sixty-seven patients underwent curative surgery that included radical prostatectomy for localised PCa between January 2000 and December 2003. None of the patients had received hormonal treatment before the operation. The characteristics of these patients are shown in Table 1. After radical prostatectomy, patients were followed by serum PSA level and imaging studies. Prostate-specific antigen relapse was defined by an elevation of serum PSA level at three consecutive measurements. Histology of the specimens was evaluated by two independent pathologists using haematoxylin- and eosin-stained tissue preparations.

Tissue samples and immunohistochemistry. All the tissue samples were fixed in 10% formalin, embedded in paraffin and cut into 4-μm-thick sections. All pathological specimens were reviewed again by genitourinary pathologists to unify the reproducibility of the diagnosis. As for the pathologic stage, all neoplasms were classified according to the 2006 TNM staging system. All study participants provided their informed consent, and the study design was approved by the ethics review board of Keio University. We carried out immunohistochemical staining for VASH1 and CD34 (as markers of vascular ECs). Tissue sections were deparaffinised in xylene, and hydrated by immersion in graded alcohols and finally in distilled water. After antigen retrieval was performed, endogenous peroxidase activity was blocked by incubation in 0.3% hydrogen peroxidase for 20 min at room temperature. The tissue sections were then incubated with a blocking solution of 5% dry milk in PBS. They were stained for 60 min at room temperature with primary antibodies, followed by staining for 30 min at room temperature with secondary antibodies. The primary antibodies were all mouse monoclonal antibodies (mAbs): anti-human VASH1 mAb diluted at 1:400 and anti-CD34 (Nichirei Biosciences, Tokyo, Japan) diluted at 1:200. We previously described a mouse mAb against a synthetic peptide corresponding to the 286–299 amino-acid sequence of VASH1 (Watanabe *et al*, 2004). The specificity of this antibody, which detects VASH1, has been documented in our previous studies (Watanabe *et al*, 2004; Yoshinaga *et al*, 2008, 2011; Hosaka *et al*, 2009; Kimura *et al*, 2009; Tamaki *et al*, 2009, 2010; Miyashita *et al*, 2012; Miyazaki *et al*, 2012). After washing with PBS, the tissue sections were incubated with secondary antibodies (Histofine Simple Stain MAX PO (M); Nichirei Biosciences). Colour was developed with 3, 3′-diaminobenzamine tetrahydrochloride in 50 mM Tris-HCl (pH 7.5) containing 0.005% hydrogen peroxide. The sections were counterstained with haematoxylin. The positive control slide CD34 antigen was prepared from paraffin-fixed bladder cancer tissue with high MVD. The appropriate negative controls slides for CD34 antigen and VASH1 were prepared by substituting the primary antibody with the immune globulin fraction of nonimmune mouse serum at the same concentration in each staining run.

Table 1. Correlation of clinicopathological parameters and MVD or VASH1 expression in the 167 study patients

Characteristic	No. of patients (%)	MVD (mean ± s.d.)	*P*-value	VASH1 density (mean ± s.d.)	*P*-value
Age (years)					
<65	99 (59.3)	133.1 ± 58.3	0.201	9.3 ± 7.4	0.101
≧65	68 (40.7)	115.6 ± 41.2		10.8 ± 7.2	
PSA					
<15	138 (82.6)	120.5 ± 47.5	0.588	9.4 ± 6.8	0.139
≧15	29 (17.4)	133.7 ± 67.9		12.3 ± 8.9	
Gleason score					
≦6	69 (41.3)	105.8 ± 42.2	<0.001	7.5 ± 5.6	<0.001
≧7	98 (58.7)	134.6 ± 54.4		11.6 ± 7.9	
Pathological Tstage					
≦pT2	113 (67.7)	111.2 ± 46.3	<0.001	8.6 ± 6.5	<0.001
≧pT3	54 (32.3)	146.8 ± 54.3		12.6 ± 8.2	

Abbreviations: MVD = microvessel density; PSA = prostate-specific antigen; VASH1 = vasohibin-1.

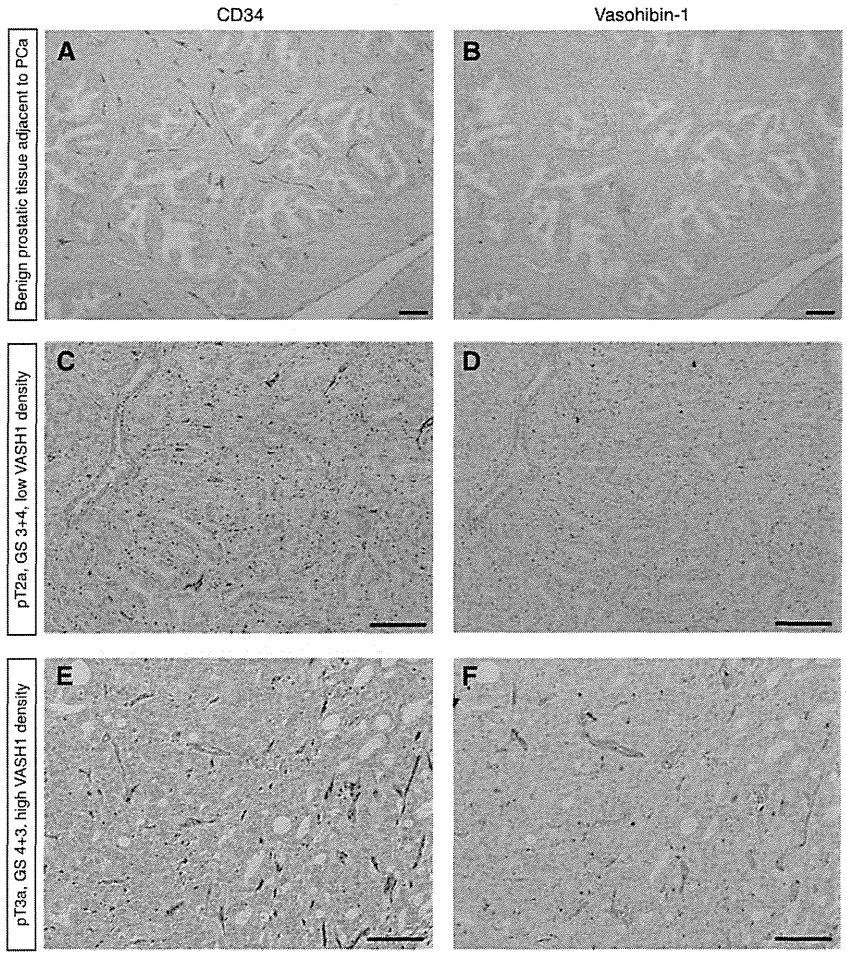

Figure 1. Immunostaining for CD34 (**A**, **C** and **E**) and VASH1 (**B**, **D** and **F**) in PCa. CD34 staining (**A**) and VASH1 staining (**B**) of vascular ECs in benign prostatic tissue adjacent to cancerous tissue. VASH1 staining of vascular ECs was negative or negligible. Low pT stage and PCa with low VASH1 density (**C** and **D**) or high pT stage with high VASH1 density (**E** and **F**). Bar = 0.1 mm.

Evaluation of immunostaining. Two authors independently evaluated immunoreactivity. They were blinded to the clinical course of the patients and the average of the numbers counted by the two investigators was used for subsequent analyses. Olympus IX71 (Olympus, Tokyo, Japan) was used for the analysis. The microvessels within the tumour were counted. Microvessels were identified based on their architecture, lumen lined by ECs and complemented by positivity of the ECs for anti-CD34 after scanning the immunostained section at low magnification ($\times 40$ and $\times 100$). The areas with the highest number of distinctly highlighted microvessels were selected, and these were counted at high magnification ($\times 200$). We evaluated at least six areas in high-power fields and selected one area with the highest number of vessels. Any immunostained EC or cluster separated from adjacent vessels was counted as a single microvessel, even in the absence of vessel lumen. Each single count was defined as the highest number of microvessels identified at the 'hot spot' as shown previously (Mikami *et al*, 2006; Kosaka *et al*, 2007; Shirotake *et al*, 2011; Yoshinaga *et al*, 2011). The highest number of microvessels in the hot spot was counted for MVD. Vasohibin-1-positive signals were counted in the 'hot spot' in which the highest number of vessels positive for anti-CD34 was identified. We regarded the number of VASH1-positive signals per mm^2 as 'VASH1 density' (Tamaki *et al*, 2009, 2010; Yoshinaga *et al*, 2011). The median values of MVD and VASH1 density were 119.5 and 9.9 per mm^2, respectively. We used a median MVD of $\geqq$120 per mm^2 and a VASH1 density of $\geqq$12 per mm^2 as the cutoff levels.

Statistical analysis. The associations between each clinicopathological parameter and VASH1 density of the tumour were analysed. These associations were validated using χ^2 test or Mann–Whitney *U*-test. Biochemical recurrence-free survival was estimated using the Kaplan–Meier method and was compared by using the log-rank test. Multivariate analysis was performed using the Cox proportional hazard model. Differences among groups were regarded as significant when $P<0.05$. These analyses were performed with the SPSS version 18.0 statistical software package (IBM corporation, New York, NY, USA).

RESULTS

Patient characteristics and VASH1 expression in PCa. Table 1 shows the clinicopathological characteristics of the patients and their association with MVD or VASH1 density in our study population. The median age of the patients was 66.6 years (range 46–75 years). Pathological T (pT) stage was $\leqq$pT2 in 113 cases (67.7%) and $\geqq$pT3 in 54 cases (32.3%). Gleason score (GS) was $\leqq$ 6 in 69 cases (41.3%) and $\geqq$7 in 98 cases (58.7%). During a median follow-up of 4.9 years, 48 patients (28.7%) experienced PSA recurrence. To elucidate the biological significance of VASH1 in PCa, we examined the expression of VASH1 by immunohistochemical staining (Figure 1). Although CD34 staining of vascular ECs in benign prostatic tissue adjacent to cancerous tissue was

Table 2. Univariate and multivariate analysis for PSA recurrence-free survival in 167 PCa patients

	Recurrence-free survival		
	Univariate	Multivariate	
Characteristic	*P*-value	HR (95%CI)	*P*-value
Age (years) <65 ≧65	0.525		
PSA	<0.001		
<15 ≧15			
Gleason score	0.073		
≦6 ≧7			
Pathological T stage	<0.001		<0.001
≦pT2 ≧pT3		4.667 (2.358-9.234)	
MVD	<0.001		
<120 per mm^2 ≧120 per mm^2			
VASH1 density	<0.001		0.007
<12 per mm^2 ≧12 per mm^2		2.950 (1.349–6.449)	

Abbreviations: CI = confidence interval; HR = hazard ratio; MVD = microvessel density; PCa = prostate cancer; PSA = prostate-specific antigen; VASH1 = vasohibin-1.

Table 3. Clinicopathological parameters in 167 patients according to the level of the VASH1 density

	No. of patients (%)		
Characteristic	Patients with VASH1 density <12 per mm^2	Patients with VASH1 density ≧12 per mm^2	*P*-value
No. of patients	83	84	
Age (years)			
<65 ≧65	53 (63.9) 30 (36.1)	46 (54.8) 38 (45.2)	0.271
PSA			
<15 ≧15	72 (86.7) 11 (13.3)	66 (78.6) 18 (21.4)	0.220
Gleason score			
≦6 ≧7	48 (57.8) 35 (42.2)	21 (25.0) 63 (75.0)	<0.001
Pathological T stage			
≦pT2 ≧pT3	65 (78.3) 18 (21.7)	48 (57.1) 36 (42.9)	0.005
MVD			
<120 per mm^2 ≧120 per mm^2	62 (74.7) 21 (25.3)	21 (25.0) 63 (75.0)	<0.001

Abbreviations: MVD = microvessel density; PSA = prostate-specific antigen; VASH1 = vasohibin-1.

positive as shown previously (Figure 1A), VASH1 staining of vascular ECs was negative or negligible (Figure 1B). Vasohibin-1 staining of vascular ECs was negative or negligible in low pT stage and low GS PCa (Figure 1D). On the other hand, in high pT stage PCa, strong VASH1 staining of vascular ECs was detected in many cases (Figure 1F). Strong VASH1 staining was observed in ECs of microvessels in the tumour lesion of high pT stage and high GS specimens. VASH1 staining of vascular ECs was negative or negligible in large-size vessels of the tumour detected by CD34.

The average MVD and VASH1 density (counts per mm^2) were 123 ± 51.6 and 9.9 ± 7.3 in 167 patients, respectively (Table 1). Patients with high GS tumours ($P<0.001$) or ≧pT3 ($P<0.001$) had significantly higher levels of both MVD and VASH1 density. As it has been reported that VASH1 associates with CD34, we also investigated the relationship between VASH1 and CD34 expression. Using Spearman's correlation coefficient test, we detected a significant positive correlation between MVD and VASH1 density in microvessels in the tumour ($\rho = 0.504$, $P<0.001$).

Prognostic significance of VASH1 expression in PCa patients. We performed univariate and multivariate analysis to determine the indicators for subsequent PSA recurrence following surgery (Table 2). Univariate analysis revealed that high PSA concentration ($P<0.001$), high pT stage ($P<0.001$), high MVD ($P<0.001$) and high VASH1 density (≧12 per mm^2) ($P<0.001$) were significant predictors of tumour recurrence. Multivariate analysis showed that high pT stage ($P<0.001$, HR = 4.667) and high VASH1 density ($P = 0.007$, HR = 2.950) were also independent predictors of PSA recurrence. A high level of MVD was not an independent predictor of PSA recurrence. Table 3 shows the association between the level of VASH1 density and clinic-pathological characteristics in 167 patients. High VASH1 density was significantly associated with GS ($P<0.001$), pT stage ($P = 0.005$) and MVD ($P<0.001$). The 5-year Kaplan–Meier PSA recurrence-free survival rate was 58.8% in patients with high VASH1 density compared with 89.1% ($P<0.001$) in their counterparts (Figure 2A).

Risk stratification for PCa according to pT stage and VASH1 density. We distributed the patients into three different groups according to pT stage and VASH1 density, which were the two statistically significant variables found by the multivariate Cox regression analysis (Figure 2C). The relative risk of death was calculated with the formula, exp (1.540 × pT stage + 1.082 × VASH1 density) for PSA recurrence-free survival. In this equation, the pT stage equaled 1 if the pT stage was pT3 or more, and it equaled 0 if the pT stage was pT2 or less. VASH1 density equaled 1 if VASH1 density was ≧12 per mm^2 and 0 if <12 per mm^2. On the basis of the relative risk of death, patients with PCa were divided into three risk groups: low (relative risk of PSA recurrence = 1), intermediate (8.02–12.7 for PSA recurrence-free survival) and high (13.8 for PSA recurrence-free survival). According to the risk stratification for PCa based on prognostic factors, 65 patients (38.9%) were in the low-risk group (low pT stage and low VASH1 density), 66 patients (39.5%) were in the high-risk group (high pT stage and high VASH1 density) and 36 patients (21.6%) were in the intermediate-risk group (all others). The 5-year PSA recurrence-free survival was 98.1% in the low-risk group, 69.7% in the intermediate-risk group and 33.7% in the high-risk group, respectively. The differences among the groups were significant ($P<0.001$ in PSA recurrence-free survival and for low- *vs* intermediate-risk group, $P<0.001$ for low- *vs* high-risk group

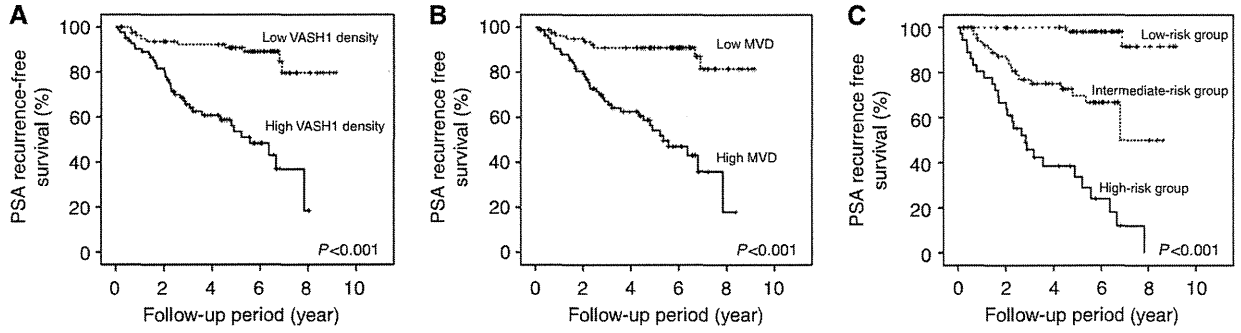

Figure 2. Kaplan–Meier curves of PSA recurrence-free survival of the patients after surgery for PCa according to VASH1 density (**A**) or MVD (**B**). Kaplan–Meier curves of PSA recurrence-free survival (**C**) of the patients after surgery for PCa according to pT stage and VASH1 density stratified according to three risk groups. Low-risk group consisted of patients with ≤pT2 and low VASH1 density. High-risk group consisted of those with ≥pT3 and high VASH1 density. All others were included in the intermediate-risk group.

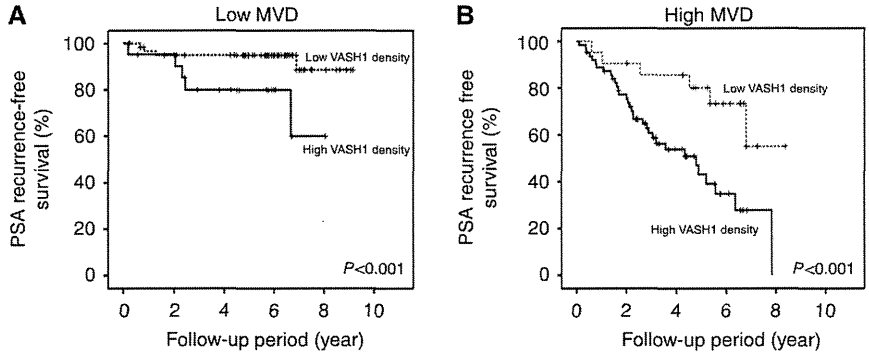

Figure 3. Kaplan–Meier curves of PSA recurrence-free survival of the patients among low (**A**) or high (**B**) MVD groups according to VASH1 density. The patients with high MVD and high VASH1 density had a significantly poorer prognosis than the counterpart group ($P<0.001$).

and $P<0.001$ for intermediate- *vs* high-risk group in PSA recurrence-free survival).

Microvessel density could be divided into two subclasses for PSA recurrence according to VASH1 density in PCa patients. Univariate analysis revealed that high MVD was one of the significant predictors of PSA recurrence (Figure 2B), while multivariate analysis showed that high MVD was not an independent predictor of PSA recurrence. Then, we re-evaluated univariate analysis of MVD according to high or low VASH1 density (Figure 3). In the low MVD group, 21 patients (25.3%) had high VASH1 density and 62 patients (74.7%) had low VASH1 density (Figure 3A). The 5-year PSA recurrence-free survival rate in the low MVD group was 79.9% for those with high VASH1 density and 94.9% for those with low VASH1 density. The difference between the groups was statistically significant ($P<0.001$). In the high MVD group, 63 patients (75.0%) had high VASH1 density and 21 patients (25.0%) had low VASH1 density (Figure 3B). The 5-year PSA recurrence-free survival rate in the high MVD group was 43.1% for those with high VASH1 density and 80.1% for those with low VASH1 density. The differences were significant ($P<0.001$). These results indicated that MVD in PCa could be subdivided into two subclasses for PSA recurrence according to VASH1 density.

DISCUSSION

In this study, we retrospectively evaluated the impact of VASH1 expression by immunohistochemical staining in a series of patients with PCa treated in a single centre. Our results suggested that VASH1 expression was a prognostic indicator in addition to other standard factors such as pT stage. High VASH1 density was related to shorter patient PSA recurrence-free survival. To the best of our knowledge, this is the first study evaluating the prognostic value of VASH1 expression in patients with prostate cancer.

Angiogenesis has a critical role in tumour growth and metastasis (Folkman, 1971; Chung *et al*, 2010). Recent studies revealed significant roles for angiogenesis in the prediction of survival in patients with different malignancies (Sato, 2003, 2012; Chung *et al*, 2010). One of the biomarkers that could reflect angiogenic aggressiveness was MVD (Weidner *et al*, 1991; Bochner *et al*, 1995; Kosaka *et al*, 2007; Shirotake *et al*, 2011). Several studies on PCa indicated that the status of MVD was associated with clinical features, such as GS and pathological stage, and could be an independent prognostic factor of patient survival (Weidner *et al*, 1993; Bettencourt *et al*, 1998; Borre *et al*, 1998; Rubin *et al*, 1999; Krupski *et al*, 2000; Josefsson *et al*, 2005; Concato *et al*, 2007, 2009; Kosaka *et al*, 2007). However, to date evidence of the prognostic role of MVD in PCa is contradictory, suggesting that the prognostic impact of MVD might be controversial. In this study, univariate analysis reveled that there was significant association between MVD and PSA recurrence. However, multivariate analysis including VASH1 density showed that MVD did not have a prognostic significance in PCa progression. One of the reasons might be because MVD corresponds to the number of accomplished vessels and includes vessels without the potential of neovascularisation in PCa. Our previous reports showed that VASH1 has been isolated from VEGF-inducible genes in ECs present in newly formed blood vessels behind the sprouting front where angiogenesis terminates (Watanabe *et al*, 2004; Sato and Sonoda, 2007; Hosaka *et al*, 2009). Recently, we have reported that histologic evidence of VASH1 expression has been found in

samples from patients with endometrial carcinoma (Yoshinaga *et al*, 2008), breast cancer (Tamaki *et al*, 2009, 2010) and cervical carcinoma (Yoshinaga *et al*, 2011). Our reports indicated that VASH1 expression was associated with tumour grade and histological type of carcinomas. Moreover, it was reported that VASH1 expression tended to be concordant with MVD, although partial dissociation was observed in some patients with breast carcinoma. VASH1 expression was significantly higher in invasive breast carcinoma, although no significant difference was observed in the level of MVD between patients with invasive disease or not (Tamaki *et al*, 2010). These studies suggested that an evaluation of the number of VASH1-positive vessels may become one of the prognostic biomarkers for metastasis and prognosis. These results indicate that VASH1 could become a new molecular biomarker of the angiogenic heterogeneity of tumours. In this study, we demonstrated that the prognostic value of MVD depends on the level of VASH1 density.

Our study demonstrated that PCa with a higher number of VASH1-positive vessels tended to have a poor prognosis. We found a significant correlation among VASH1 density, GS and pT stage. Multivariate analysis showed that high VASH1 density was an independent prognostic factor, suggesting that the status of VASH1 density could serve as a biomarker of the malignant potential of tumour angiogenesis. These results suggest that the level of VASH1 expression may influence the clinical course of prostate cancer progression. Moreover, VASH1 may become a molecular target in PCa patients.

Using VASH1 density and other independent indicators, we established a prognostic risk stratification for PCa. Patients were stratified into three groups according to statistical modelling based on the relative risk associated with the prognostic indicators derived from multivariate analysis. As shown in Figure 2C among patients with PCa, the prognosis of patients with higher pT stage and high VASH1 density was worse than that of the other groups ($P<0.001$). This stratification made it possible to predict PSA recurrence more accurately, suggesting more appropriate follow-up including PSA follow-up interval.

In conclusion, these results indicated that VASH1 can serve as a new biomarker for predicting PCa progression and could become a molecular target in PCa, especially for targeting tumour angiogenesis.

ACKNOWLEDGEMENTS

We thank colleagues from the Department of Vascular Biology, Institute of Development, Aging and Cancer, Tohoku University for their excellent technical assistance in purifying anti-human VASH1 mAb. This work was supported in part by grants-in-aid for Scientific Research from the Ministry of Education, Culture, Sports, Science, and Technology of Japan, by the Prostate Research Fund in Japan, the Japan Urological Association (5th Young Research Grant 2011 to TK) and the Cooperative Research Project Program 2011, 2012 of Joint Usage/Research Center at the Institute of Development, Aging and Cancer, Tohoku University.

CONFLICT OF INTEREST

The authors declare no conflict of interest.

REFERENCES

Bettencourt MC, Bauer JJ, Sesterhenn IA, Connelly RR, Moul JW (1998) CD34 immunohistochemical assessment of angiogenesis as a prognostic marker for prostate cancer recurrence after radical prostatectomy. *J Urol* **160**: 459–465.

Bochner BH, Cote RJ, Weidner N, Groshen S, Chen SC, Skinner DG, Nichols PW (1995) Angiogenesis in bladder cancer: relationship between microvessel density and tumor prognosis. *J Natl Cancer Inst* **87**: 1603–1612.

Borre M, Offersen BV, Nerstrom B, Overgaard J (1998) Microvessel density predicts survival in prostate cancer patients subjected to watchful waiting. *Br J Cancer* **78**: 940–944.

Chen Y, Sawyers CL, Scher HI (2008) Targeting the androgen receptor pathway in prostate cancer. *Curr Opin Pharmacol* **8**: 440–448.

Chung AS, Lee J, Ferrara N (2010) Targeting the tumour vasculature: insights from physiological angiogenesis. *Nat Rev Cancer* **10**: 505–514.

Concato J, Jain D, Li WW, Risch HA, Uchio EM, Wells CK (2007) Molecular markers and mortality in prostate cancer. *BJU Int* **100**: 1259–1263.

Concato J, Jain D, Uchio E, Risch H, Li WW, Wells CK (2009) Molecular markers and death from prostate cancer. *Ann Intern Med* **150**: 595–603.

Folkman J (1971) Tumor angiogenesis: therapeutic implications. *N Engl J Med* **285**: 1182–1186.

Hosaka T, Kimura H, Heishi T, Suzuki Y, Miyashita H, Ohta H, Sonoda H, Moriya T, Suzuki S, Kondo T, Sato Y (2009) Vasohibin-1 expression in endothelium of tumor blood vessels regulates angiogenesis. *Am J Pathol* **175**: 430–439.

Jemal A, Siegel R, Xu J, Ward E (2010) Cancer statistics, 2010. *CA Cancer J Clin* **60**: 277–300.

Josefsson A, Wikstrom P, Granfors T, Egevad L, Karlberg L, Stattin P, Bergh A (2005) Tumor size, vascular density and proliferation as prognostic markers in GS 6 and GS 7 prostate tumors in patients with long follow-up and non-curative treatment. *Eur Urol* **48**: 577–583.

Kimura H, Miyashita H, Suzuki Y, Kobayashi M, Watanabe K, Sonoda H, Ohta H, Fujiwara T, Shimosegawa T, Sato Y (2009) Distinctive localization and opposed roles of vasohibin-1 and vasohibin-2 in the regulation of angiogenesis. *Blood* **113**: 4810–4818.

Kosaka T, Miyajima A, Takayama E, Kikuchi E, Nakashima J, Ohigashi T, Asano T, Sakamoto M, Okita H, Murai M, Hayakawa M (2007) Angiotensin II type 1 receptor antagonist as an angiogenic inhibitor in prostate cancer. *Prostate* **67**: 41–49.

Krupski T, Petroni GR, Frierson Jr. HF, Theodorescu JU (2000) Microvessel density, p53, retinoblastoma, and chromogranin A immunohistochemistry as predictors of disease-specific survival following radical prostatectomy for carcinoma of the prostate. *Urology* **55**: 743–749.

Mikami S, Oya M, Mizuno R, Murai M, Mukai M, Okada Y (2006) Expression of Ets-1 in human clear cell renal cell carcinomas: implications for angiogenesis. *Cancer Sci* **97**: 875–882.

Miyashita H, Watanabe T, Hayashi H, Suzuki Y, Nakamura T, Ito S, Ono M, Hoshikawa Y, Okada Y, Kondo T, Sato Y (2012) Angiogenesis inhibitor vasohibin-1 enhances stress resistance of endothelial cells via induction of SOD2 and SIRT1. *PLoS One* **7**: e46459.

Miyazaki Y, Kosaka T, Mikami S, Kikuchi E, Tanaka N, Maeda T, Ishida M, Miyajima A, Nakagawa K, Okada Y, Sato Y, Oya M (2012) The prognostic significance of vasohibin-1 expression in patients with upper urinary tract urothelial carcinoma. *Clin Cancer Res* **18**: 4145–4153.

Rubin MA, Buyyounouski M, Bagiella E, Sharir S, Neugut A, Benson M, de la Taille A, Katz AE, Olsson CA, Ennis RD (1999) Microvessel density in prostate cancer: lack of correlation with tumor grade, pathologic stage, and clinical outcome. *Urology* **53**: 542–547.

Sato Y (2003) Molecular diagnosis of tumor angiogenesis and anti-angiogenic cancer therapy. *Int J Clin Oncol* **8**: 200–206.

Sato Y, Sonoda H (2007) The vasohibin family: a negative regulatory system of angiogenesis genetically programmed in endothelial cells. *Arterioscler Thromb Vasc Biol* **27**: 37–41.

Sato Y (2012) The vasohibin family: Novel regulators of angiogenesis. *Vascul Pharmacol* **56**: 262–266.

Scher HI, Sawyers CL (2005) Biology of progressive, castration-resistant prostate cancer: directed therapies targeting the androgen-receptor signaling axis. *J Clin Oncol* **23**: 8253–8261.

Shirotake S, Miyajima A, Kosaka T, Tanaka N, Maeda T, Kikuchi E, Oya M (2011) Angiotensin II type 1 receptor expression and microvessel density in human bladder cancer. *Urology* **77**: 1009, e19–e25.

Tamaki K, Moriya T, Sato Y, Ishida T, Maruo Y, Yoshinaga K, Ohuchi N, Sasano H (2009) Vasohibin-1 in human breast carcinoma: a potential negative feedback regulator of angiogenesis. *Cancer Sci* **100**: 88–94.

Tamaki K, Sasano H, Maruo Y, Takahashi Y, Miyashita M, Moriya T, Sato Y, Hirakawa H, Tamaki N, Watanabe M, Ishida T, Ohuchi N (2010) Vasohibin-1 as a potential predictor of aggressive behavior of ductal carcinoma *in situ* of the breast. *Cancer Sci* **101**: 1051–1058.

Watanabe K, Hasegawa Y, Yamashita H, Shimizu K, Ding Y, Abe M, Ohta H, Imagawa K, Hojo K, Maki H, Sonoda H, Sato Y (2004) Vasohibin as an endothelium-derived negative feedback regulator of angiogenesis. *J Clin Invest* **114**: 898–907.

Weidner N, Semple JP, Welch WR, Folkman J (1991) Tumor angiogenesis and metastasis – correlation in invasive breast carcinoma. *N Engl J Med* **324**: 1–8.

Weidner N, Carroll PR, Flax J, Blumenfeld W, Folkman J (1993) Tumor angiogenesis correlates with metastasis in invasive prostate carcinoma. *Am J Pathol* **143**: 401–409.

Yoshinaga K, Ito K, Moriya T, Nagase S, Takano T, Niikura H, Sasano H, Yaegashi N, Sato Y (2011) Roles of intrinsic angiogenesis inhibitor, vasohibin, in cervical carcinomas. *Cancer Sci* **102**: 446–451.

Yoshinaga K, Ito K, Moriya T, Nagase S, Takano T, Niikura H, Yaegashi N, Sato Y (2008) Expression of vasohibin as a novel endothelium-derived angiogenesis inhibitor in endometrial cancer *Cancer Sci* **99**: 914–919.

OPEN ACCESS Freely available online

PLOS | ONE

An Angiogenic Role for Adrenomedullin in Choroidal Neovascularization

Susumu Sakimoto[1,2], Hiroyasu Kidoya[1], Motohiro Kamei[2], Hisamichi Naito[1], Daishi Yamakawa[1], Hirokazu Sakaguchi[2], Taku Wakabayashi[1,2], Kohji Nishida[2], Nobuyuki Takakura[1,3]*

1 Department of Signal Transduction, Research Institute for Microbial Diseases, Osaka University, Suita, Osaka, Japan, **2** Department of Ophthalmology, Osaka University Graduate School of Medicine, Suita, Osaka, Japan, **3** JST(Japan Science and Technology Agency), CREST, Tokyo, Japan

Abstract

Purpose: Adrenomedullin (ADM) has been shown to take part in physiological and pathological angiogenesis. The purpose of this study was to investigate whether ADM signaling is involved in choroidal neovascularization (CNV) using a mouse model.

Methods and Results: CNV was induced by laser photocoagulation in 8-week-old C57BL/6 mice. ADM mRNA expression significantly increased following treatment, peaking 4 days thereafter. The expression of ADM receptor (ADM-R) components (CRLR, RAMP2 and RAMP 3) was higher in $CD31^{+}CD45^{-}$ endothelial cells (ECs) than $CD31^{-}CD45^{-}$ non-ECs. Inflammatory stimulation upregulated the expression of ADM not only in cell lines but also in cells in primary cultures of the choroid/retinal pigment epithelium complex. Supernatants from TNFα-treated macrophage cell lines potentiated the proliferation of ECs and this was partially suppressed by an ADM antagonist, ADM (22–52). Intravitreous injection of ADM (22–52) or ADM neutralizing monoclonal antibody (mAb) after laser treatment significantly reduced the size of CNV compared with vehicle-treated controls ($p<0.01$).

Conclusions: ADM signaling is involved in laser-induced CNV formation, because both an ADM antagonist and ADM mAb significantly inhibited it. Suppression of ADM signaling might be a valuable alternative treatment for CNV associated with age-related macular degeneration.

Citation: Sakimoto S, Kidoya H, Kamei M, Naito H, Yamakawa D, et al. (2013) An Angiogenic Role for Adrenomedullin in Choroidal Neovascularization. PLoS ONE 8(3): e58096. doi:10.1371/journal.pone.0058096

Editor: Tailoi Chan-Ling, University of Sydney, Australia

Received March 30, 2012; **Accepted** February 3, 2013; **Published** March 8, 2013

Funding: This work was supported by a grant from the Ministry of Education, Science, Sports, and Culture of Japan. The funders had no role in study design, data collection and analysis, decision to publish.

Competing Interests: The authors have declared that no competing interests exist.

* E-mail: ntakaku@biken.osaka-u.ac.jp

Introduction

Aberrant angiogenesis occurs under numerous pathological conditions, such as cancer, rheumatoid arthritis, psoriasis and many ocular diseases. Age-related macular degeneration (AMD) is the leading cause of vision loss in elderly persons in developed countries. Patients with severe vision loss are often affected by wet AMD [1] the central pathologic features of which are recognized as choroidal neovascularization (CNV), induced by a complex pathogenic process whereby new blood vessels are generated from the choriocapillaris beneath the retina. CNV-associated vessels tend to leak and bleed, thereby severely affecting the neural tissue of the macula.

Genetic variation in complement factor genes in AMD patients suggests inflammatory processes as a trigger of drusen formation which is a hallmark of this disease. Moreover, infiltration of inflammatory cells such as macrophages which produce various angiogenic factors could support neovessel formation from the choriocappillaris directly and indirectly [2,3,4,5].

Adrenomedullin (ADM), identified as a potent vasodilator with wide tissue distribution, is a multifunctional 52 amino acid peptide activating heterodimeric receptors composed of a seven transmembrane (7TM) G-protein-coupled receptor (GPCR) calcitonin-receptor-like receptor (CRLR, now known as CL) [6] and receptor activity-modifying proteins (RAMPs) [7]. ADM is also thought to play a critical role in forming blood vessels, with functions including regulation of vascular stability under both physiological and pathological conditions [8–10]. Gene targeting analysis in mice showed that global deletion of the ADM gene results in embryonic lethality at E13.5 caused by vascular abnormalities [10].

Expression of ADM is regulated by hypoxia, growth factors and inflammation [6,8]. Moreover, accumulating evidence for the involvement of ADM in tumor angiogenesis has demonstrated that inhibition of ADM function by neutralizing antibody or the ADM antagonist ADM (22–52) inhibits tumor growth in xenograft models [11,12,13]. In vascular endothelial cells (ECs), activation of phosphatidylinositol 3′ kinase (PI3K/Akt), mitogen-activated protein kinase (MAPK) and focal adhesion kinase (p125FAK) plays a role in ADM-induced angiogenesis [8,14,15]. The level of ADM expression in tumors correlates with vascular density in patients [16] and ADM-heterozygous knockout mice have reduced neovascularization in a tumor xenograft model [9].

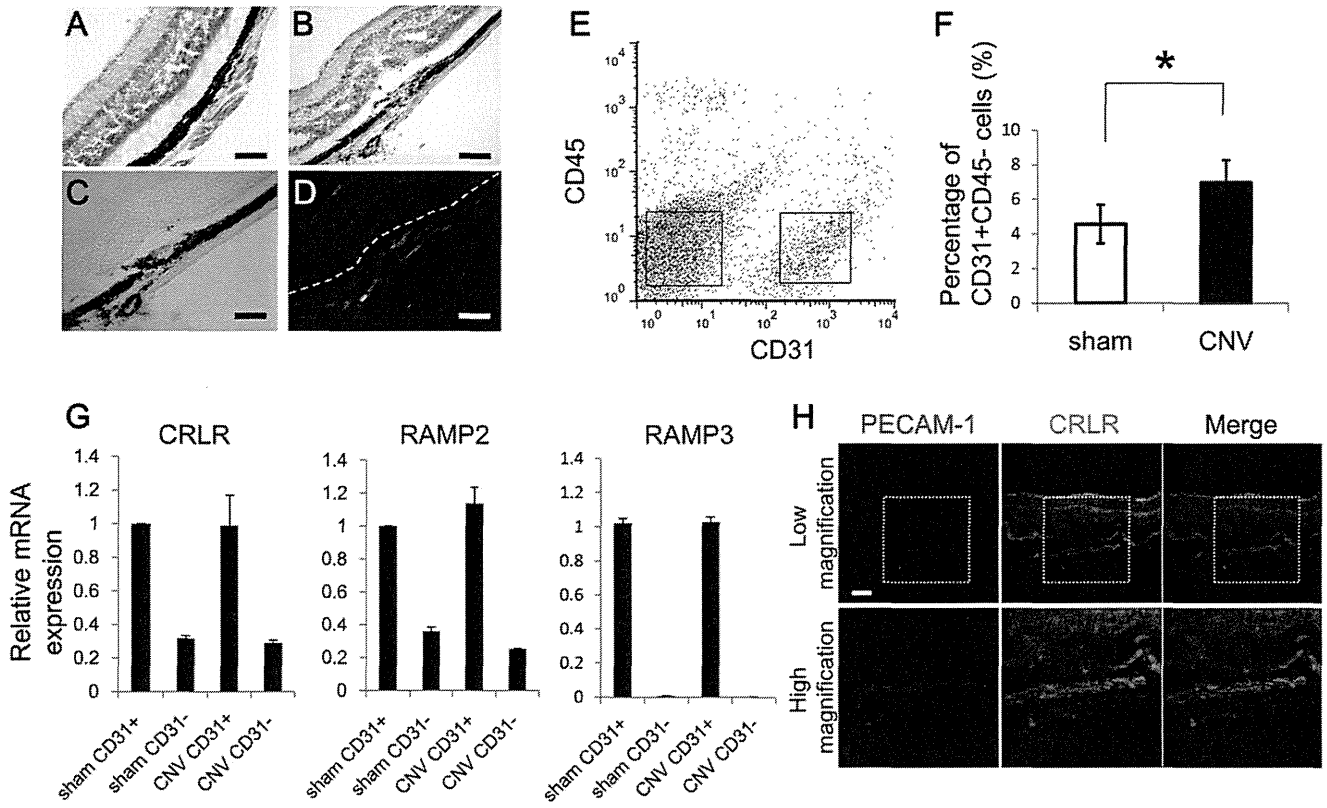

Figure 1. Expression of ADM receptors in choroidal ECs. (A, B) Hematoxylin-eosin-stained light micrograph of normal eye (A) and CNV lesion 7 days after laser treatment (B). Bar, 100 μm. (C) Light micrograph of serial sections of (B). Bar, 100 μm. (D) Immunohistochemistry of (C) with anti-PECAM-1/CD31 antibody. Dotted line indicates the borderline between the neural retina and RPE. Because the CNV lesion did not invade into the retina in this model, we could sort the ECs not from nerural retina but from CNV lesions and choroidal tissue in the following flow cytometry experiments. Bar, 100 μm. (E) Flow cytometric analysis of choroidal ECs from wild-type mice. $CD31^+CD45^-$ cells gated on the right are designated as ECs. (F) Quantitative evaluation of the percentage of choroidal EC 7 days after laser treatment. The number was calculated per cell total ($n = \geq 5$, $^*P<0.05$). (G) qRT–PCR analysis of ADM receptor component expression in choroidal ECs. The value in $CD31^+CD45^-$ ECs was compared with that in $CD31^-CD45^-$ non-ECs sorted as gated in (A). Note that the expression level of ADM receptors is not significantly different between ECs and non-ECs in both sham-operated mice (sham) and laser-irradiated CNV mice (CNV). (H) Immunostaining of the CNV 7 days after laser treatment with anti-PECAM-1 (red) and anti-CRLR (green) antibody. High maginification indicate the dotted box in Low magnification. Bar, 100 μm.
doi:10.1371/journal.pone.0058096.g001

However, it is poorly understood whether ADM could be an effector in other disease models, especially in ocular neovascularization. Therefore, here we investigate whether ADM has a role in proangiogenesis in laser-induced CNV, which is widely accepted as a mammalian AMD model, and have attempted to characterize mechanisms of ADM signaling in CNV formation.

Materials and Methods

Animals

All experiments were conducted under the applicable laws and guidelines for the care and use of laboratory animals in the Research Institute for Microbial Diseases, Osaka University, approved by the Animal Experiment Committee of the Research Institute for Microbial Disease, Osaka University.

Laser-induced CNV and Drug Treatment

Laser photocoagulation (514 nm Argon laser, 150 mW, 50 ms duration, 50 mm spot size; Ultima 2000 SE, Lumenis/Coherent) was performed bilaterally in each 8-week-old wild-type C57BL/6 mouse. A total of 6 laser spots per eye were created in a standard fashion around the optic nerve using a slit lamp delivery system (Carl Zeiss, Germany) and using a cover slip as a contact lens. Only burns that produced a bubble, indicating rupture of the Bruch membrane, were included in the study. Eyes merely touched with a cover slip acted as sham-operated controls. Immediately after laser photocoagulation, mice were randomized into several groups and received intravitreal injections of 1 μl ADM (22–52) (10 μM or 100 μM), ADM (200 μM) (Peptide Institute, Osaka, Japan), SU1498 (10 μM) [17], ADM monoclonal antibody (1.45 mg/ml) (provided by Diagnostic Science Division, Shionogi & Co., Ltd.) or vehicle (PBS). The same treatment was performed 3 days after photocoagulation in the same fashion. Intravitreal injection was performed with the FemtoJet Microinjector System (Eppendorf, Germany) under a high magnification stereomicroscope (Leica M125, Germany). Eyes were enucleated and fixed for immunohistochemistry 7 days after photocoagulation. We used 16 mice and 16 choroidal flatmounts in ADM antagonist experiments, 8 mice and 8 flatmounts in experiments using combination treatment with ADM antagonist and VEGF inhibitor, and 10 mice and 10 flatmounts in ADM mAb experiments.

Measurement of Laser-induced CNV Size

On day 7 after laser photocoagulation, the sizes of CNV lesions were measured on RPE-choroid flat mounts as described pre-

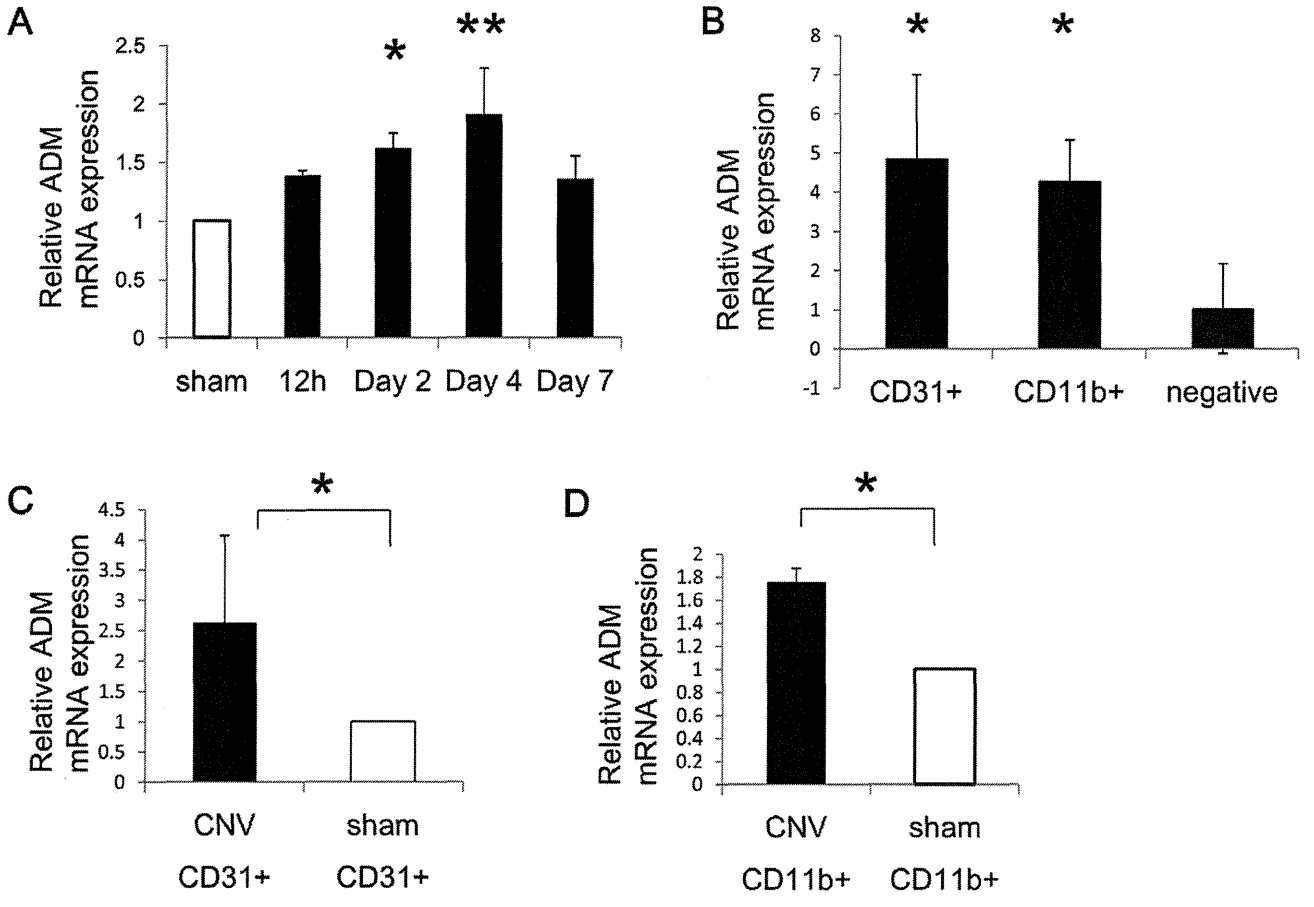

Figure 2. ADM expression after laser treatment. (A) Time course ADM mRNA expression by qRT–PCR analysis in the RPE/choroid complex after laser treatment. Results are shown as fold-increase in comparison with RPE/choroid complexes from sham-operated eyes. (B) qRT–PCR analysis of ADM mRNA expression in sorted CD31$^+$ cells (EC-enriched cell population), CD11b$^+$ cells (monocyte/macrophage lineage cells) and cells negative for either CD31 or CD11b (non-EC, non-monocyte/macrophage lineage fraction) 3 days after laser treatment ($n \geq 5$). (C) qRT–PCR analysis of ADM mRNA expression in sorted CD31$^+$ cells after laser treatment (CNV) compared to sham-treated eyes (sham). ($n \geq 5$, *$P<0.05$) (D) qRT–PCR analysis of ADM mRNA expression in sorted CD11b$^+$ cells after laser treatment compared to sham-treated eyes. ($n \geq 5$, *$P<0.05$).
doi:10.1371/journal.pone.0058096.g002

viously [18]. Image J for Windows (NIH, Bethesda, Maryland) analysis software was used to measure the area of CNV, with the operator blinded with respect to treatment groups.

Flow Cytometry (Analysis and Cell Sorting)

Procedures for cell preparation and staining were as previously reported [19]. Briefly, eyes from at least 5 mice which were laser coagulated or not were extracted and the RPE-choroid complex were gently scraped off the sclera. The RPE-complex was digested with collagenase (Wako, Osaka, Japan), and type II collagenase (Worthington Biochemical Corp., Lakewood, New Jersey) at 37°C. The digested tissue was passed through 40-μm filters to yield single cell suspensions. Cell surface antigen staining was performed as described previously [20]. Anti-CD45, -CD31, -CD11b (Pharmingen, BD Biosciences) mAbs were used for immunofluorescence staining. The stained cells were analyzed and sorted using a FACSAria flow cytometer (BD) with FlowJo (TreeStar) software. Dead cells were excluded from the analyses using the 2D profile of forward versus side scatter.

Quantitative Reverse-transcription Real-time PCR (qRT-PCR)

For RNA extraction, we used at least 5 mice in each group for sorted cells as indicated above. For analysis of ADM mRNA expression in RPE/choroid complexes, we used 2 mice per day. RNA was extracted from cells using an RNeasy Mini Kit (Qiagen), and cDNA was generated using reverse transcriptase from the ExScript RT reagent Kit (Perfect Real Time) (Takara). Real-time PCR was performed using a Stratagene Mx3000P (Stratagene, La Jolla, CA). Polymerase chain reaction (PCR) was performed on cDNA using specific primers following; mouse CRLR, 5′-ACC TGC ACA CAC TCA TCG TG-3′ and 5′-TGA TCC AGC AAT TGT CGT TG-3′; mouse RAMP2, 5′-CTG AGG ACA GCC TTG TGT CA-3′ and 5′-AAG TCC AGT TGC ACC AGT CC-3′; mouse RAMP3, 5′-AAG GTG GCT GTC TGG AAG TG-3′ and 5′-TGA TGT TGG TCT CCA TCT CG′; mouse ADM, 5′- GAC TCG CTG ATG AGA CGA CA-3′ and 5′- GAA CCC TGG TTC ATG CTC TG′; mouse GAPDH, 5′-TGG CAA AGT GGA GAT TGT TGC C-3′ and 5′- AAG ATG GTG ATG GGC TTC CCG-3′; human ADM, 5′- ATG AAG GGT GCC TCT CGA A-3′ and 5′- CCC TGG AAG TTG TTC ATG C-3′; human GAPDH, 5′- GAA GGT GAA GGT CGG AGT C-3′ and 5′- GAA GAT GGT GAT GGG ATT TC-3′.

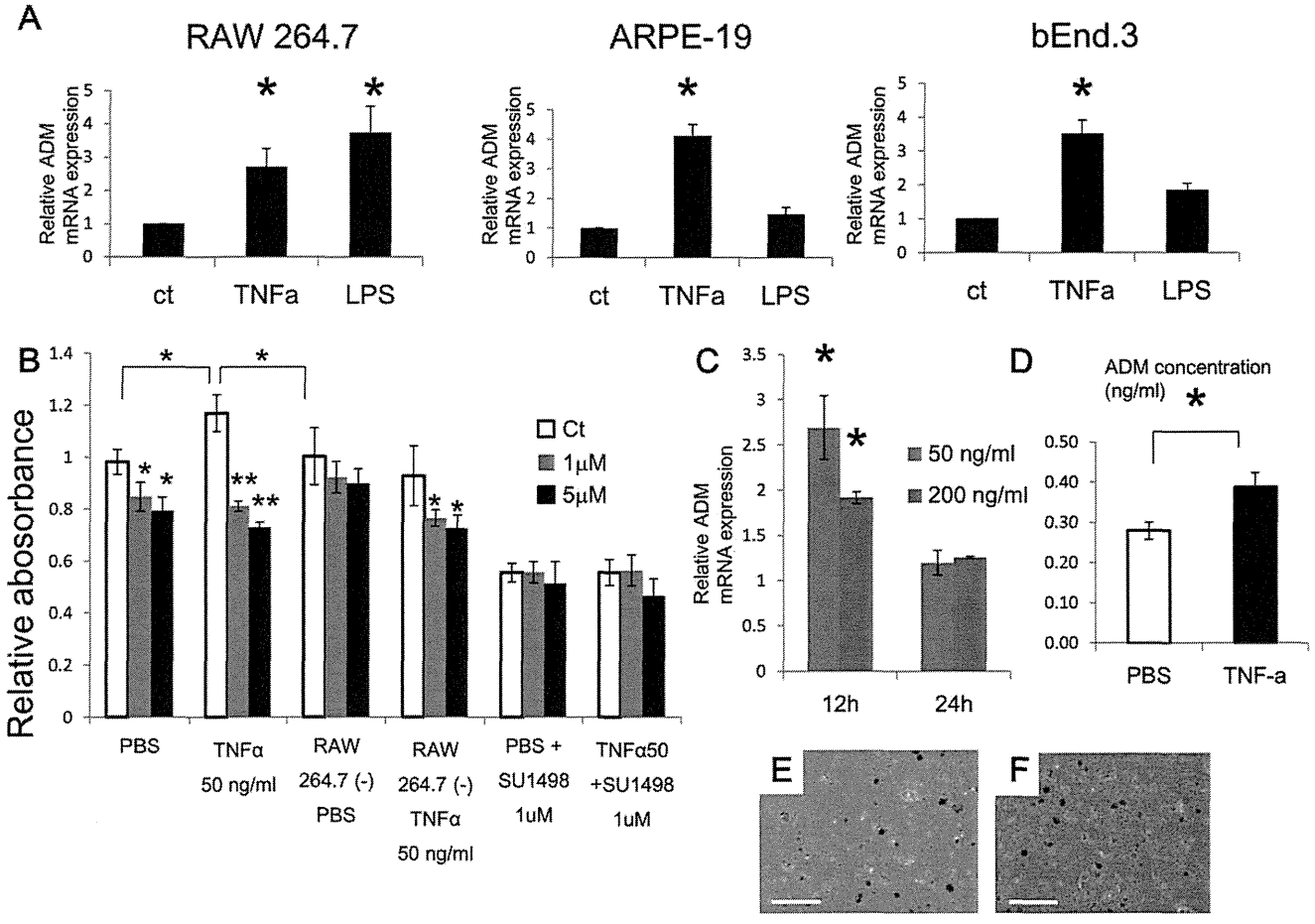

Figure 3. In vitro effect of an ADM antagonist. (A) qRT–PCR analysis of ADM mRNA expression after 12 hr TNF-α or LPS stimulation of cells, as indicated (n = 3, *P<0.01). (B) EC proliferation assay using bEND.3 which was incubated with or without supernatant from TNF-α-stimulated RAW 264.7 in the presence or absence of the ADM antagonist ADM (22–52). The white bar indicates the PBS group, gray indicates the 1 μM ADM (22–52) group and black the 5 μM ADM (22–52) group. ECs in all groups were incubated with supernatant from RAW 264.7 cells except for RAW 264.7 (-) groups (culture medium without supernatant of RAW 264.7 cells). 1 μM SU1498 was added to indicated groups (n = 3, **P<0.01, *P<0.05). (C) qRT–PCR analysis of ADM mRNA expression after 12 and 24 hr TNF-α stimulation of primary RPE/choroid cultures (n = 3, *P<0.05). (D) ELISA of secreted ADM from primary RPE/choroid cultures after stimulation with 50 ng/ml TNF-α or culture with PBS alone (*P<0.05) (E, F) Appearance of primary RPE/choroid cultures after stimulation with PBS (E) or 50 ng/ml TNF-α(F). Scale bar: 100 μm.
doi:10.1371/journal.pone.0058096.g003

Expression level of the target gene was normalized to the GAPDH level in each sample.

In vitro Assays

We examined the in vitro effect of ADM on inflammatory responses of 3 major cell types associated with CNV formation, i.e., microvascular ECs, macrophages, and RPE cells, using the murine cell lines bEnd3, RAW264.7, and the human cell line ARPE-19, respectively. ARPE19 cells were purchased from the American Type Culture Collection (ATCC, Manassas, VA). Cells were cultured in six-well plates for 12 hours in DMEM (Sigma, ATCC and Nikken, respectively). After 4 hours serum starvation using 0.5% fetal bovine serum (FBS), cells were stimulated with tumor necrosis factor (TNF)-α (PeproTech, 50 ng/mL) or lipopolysaccharide (LPS; Wako, 10 μg/mL). After a 12 hour incubation, cell lysate from each line, and the supernatants from cultures of RAW264.7 cells, were processed for real-time RT PCR and EC proliferation assays, respectively. ECs (bEnd3) which were incubated for an additional 4 hours with supernatant plus 1 μM or 5 μM ADM (22–52), or PBS, were quantified using Cell-counting kit-8 (DOJINDO) according to the supplier's protocol. 1 μM SU1498 was added to the supernatant in some experiments. Dose-response model assessing the toxicity of ADM (22–52) was also performed using same kit after 24 hour incubation of ADM inhibitor at indicated concentration. Absorbance was then measured at 490 nm, and at 630 nm as reference, with a Microplate Reader 550 (Bio-Rad Laboratories). Primary culture of RPE/choroid complexes was performed using cells dissected from 8-week-old wild-type C57BL/6 mice. Tissues were dissociated with trypsin, resuspended in DMEM containing 20% FBS and then plated on laminin-coated 24-well plates at a density of a tissue from1 mouse/well and incubated at 37°C, 5% CO_2 for 24 h before 4 hours serum starvation with 0.5% FBS. After 12 hours TNF-α treatment, tissues were collected and immediately washed with PBS before RNA extraction. For ELISA, after seeding the primary culture, we cultured for 24 hours as indicated above, then serum-starved for 4 hours in DMEM without FBS before TNF-α stimulation. We stimulated cells with 50 ng/ml TNF-α for 24 hours without FBS. We used an ADM detection kit (Phoenix Pharmaceuticals) according to the supplier's protocol.

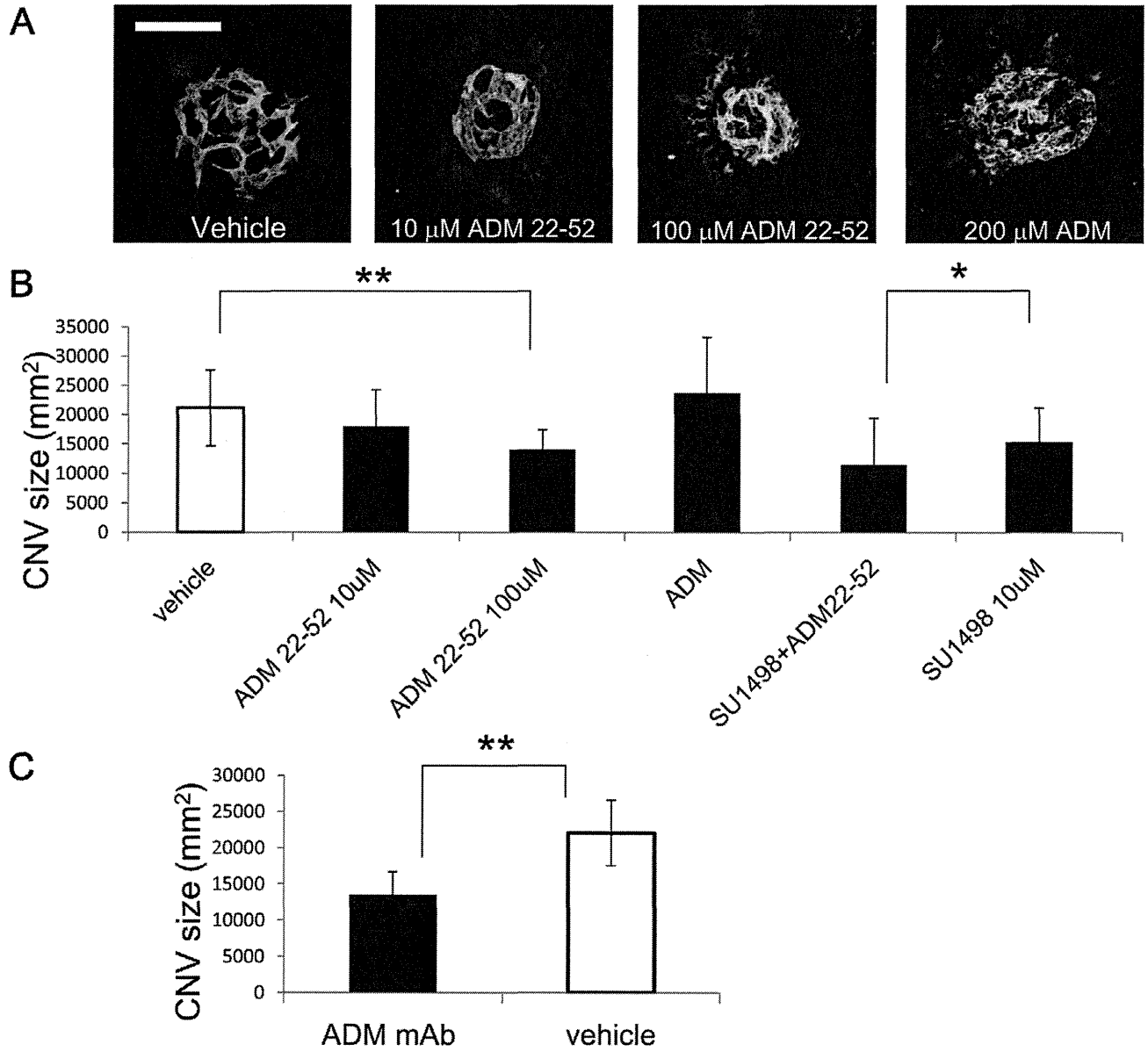

Figure 4. Suppression of CNV in mice by blocking ADM. (A) Flat-mount immunofluorescence staining with anti-PECAM-1/CD31 antibody in the choroid after vehicle, ADM (22–52) or recombinant ADM treatment. Scale bar: 100 μm. (B) Quantitative analysis of CNV size as revealed in (A). (n = 16, **P<0.01) and quantitative analysis of CNV size after treatment with 10 μM SU1498 with or without 100 μM ADM (22–52) (n = 8, *P<0.05). (C) Quantitative analysis of CNV size treated with ADM mAb compared to vehicle. (n = 10, **P<0.01). Error bars indicate mean ± s.d.
doi:10.1371/journal.pone.0058096.g004

Immunohistochemistry

The procedure for tissue preparation and staining was as previously reported [21]. For immunohistochemistry, biotin-conjugated anti-CD31 antibody (BD Biosciences, 1:200) was used for staining and anti-rat IgG Alexa Fluor 488 (Invitrogen, 1:300) as the secondary antibody. Samples were visualized using DM5500B (Leica) and confocal microscopy (TCS/SP5, Leica). Images were acquired with a DFC 500 digital camera (Leica) and processed with the Leica application suite (Leica) and Adobe Photoshop CS3 software (Adobe systems). All images shown are representative of more than 6 independent experiments.

Statistical Analysis

All data are presented as mean ± standard error of the mean (SEM). For statistical analysis, the statcel 2 software package (OMS) was used. In experiments involving qRT-PCR and CNV suppression with ADM mAb, we used two-sided Student's t-test to compare two groups (except for expression of ADM mRNA after CNV induction).We used analysis of variance performed on all data followed by Tukey–Kramer multiple comparison testing in qRT-PCR experiments for expression of ADM mRNA after CNV induction, EC proliferation assays using bEND.3 and for experiments on CNV suppression with ADM and VEGF antagonists. A probability value of less than 0.05 was considered statistically significant.

Results

To elucidate the involvement of ADM signaling in CNV, we first investigated the expression of the ADM receptor in choroidal vascular ECs in the CNV model. After we confirmed that CNV did not invade retinal tissue (Fig. 1A–D), $CD31^+CD45^-$ ECs in the RPE-choroid complex were analyzed by flow cytometry (Fig. 1E) and their number was calculated as a percentage of a total of 5×10^4 choroid/RPE complex cells 7 days after laser induction. We confirmed that the number of ECs increases after induction of CNV in laser-treated eyes (6.96% of total cells) compared to control eyes (4.57% of total cells) (Fig. 1F). There was no change in the number of $CD31^+$ $CD45^+$ or $CD31^-CD45^+$ cells; however, CD11b cells increased after laser-induction of CNV (6.32% vs 1.8%) (data not shown). Because ADM signaling is known to be mediated through CRLR/RAMP2 and CRLR/RAMP3 receptors, we analyzed the expression of CRLR, RAMP2 and RAMP3 mRNA in choroid/RPE complexes after induction of CNV. CRLR, RAMP2 and RAMP3 were highly expressed in the $CD31^+CD45^-$ ECs compared to $CD31^-CD45^-$ non-ECs. However, the level of expression of these ADM receptor components in ECs was not altered after CNV induction compared to sham-operated control groups (Fig. 1G). Moreover, we confirmed the expression of CRLR in the ECs of CNV by immunostaining (Fig. 1H).

Next, we assessed the expression of ADM during CNV formation. In the laser-induced CNV model, the presence of different angiogenic factors in RPE-Choroid complexes has already been reported [22]. We analyzed the expression of ADM mRNA and found that it increased in a time-dependent fashion and peaked 4 days after laser treatment (Fig. 2A). Because it is reported that ADM promotes angiogenesis in both an autocrine and a paracrine manner [8,23], we focused on two cell populations which could be isolated by flow cytometry: $CD31^+$ ECs and $CD11b^+$ monocytes/macrophages. We confirmed that both ECs and macrophages express more ADM mRNA compared to $CD31^-CD11b^-$ cells (Fig. 2B). Furthermore, after CNV induction, ADM expression was significantly upregulated in both ECs and macrophages compared to the same cells in sham-operated mice (Fig. 2C, D). Therefore, these data suggest that ADM is involved in this laser-induced CNV model.

It is well known that inflammatory cytokines upregulate ADM expression in various cells [24,25,26]. We confirmed this by using macrophage (RAW264.7), EC (bEnd.3), and retinal pigment epithelial (ARPE-19) cell lines stimulated with TNF-α and LPS (Fig. 3A). It has been reported that ADM induces EC proliferation, migration and tube formation through phosphatidylinositol 3′ kinase (PI 3′ -kinase)/Akt, extracellular signal-regulated kinase (ERK), and tyrosine phosphorylation of focal adhesion kinase (p125 FAK) [14]. Thus, we tested whether culture supernatant from RAW264.7 cells after TNF-α stimulation promotes EC proliferation and whether this can be inhibited by a widely-accepted ADM antagonist, ADM (22–52) [27]. Although the inhibitory effect was weak compared to a potent VEGF-A signaling inhibitor, SU1498 [28], ADM (22–52) did significantly suppress proliferation of EC cultured not only in supernatant from TNF-α-stimulated macrophages but also to some extent in medium containing TNF-α without macrophages (Fig. 3B). Additionally, we confirmed the absence of the potential toxicity of ADM (22–52) using an in vitro dose-response model (Fig. S1). These data suggest that ADM signaling affects EC proliferation in an autocrine and a paracrine manner. Moreover, we evaluated the expression of ADM in 24 hour-cultured primary RPE/choroid complexes obtained from wild-type mice. TNF-α stimulation of cultured primary RPE/choroid complexes significantly upregulated ADM mRNA and protein levels at the 12 hour time point (Fig. 3C and 3D); however, expression of ADM mRNA after 24 hours was downregulated relative to the 12 hour time point (Fig. 3C). The morphology of the cells did not change(Fig. 3E and 3F).

To clarify the role of ADM in this CNV model, we inhibit ADM signaling using intraocular injections of ADM antagonist, ADM (22–52). Quantification of CNV size judged by immunohistochemical analysis with anti-PECAM-1 Ab 7 days after laser treatment revealed that intraocular injection of ADM (22–52) significantly inhibited the formation of CNV to approximately 60% of controls. In contrast, injection of recombinant ADM did not affect the size of CNV compared to controls, contrary to our expectations (Fig. 4A and B). This suggests that an excessive amount of ADM is produced in the choroid/RPE in this CNV model. Next, we assessed whether the ADM antagonist had any synergistic effect with SU1498 on CNV. Treatment with ADM antagonist and SU1498 together suppressed CNV formation more than SU1498 alone (Fig. 4C). Furthermore, we confirmed the effect of anti-ADM monoclonal antibody; intraocular injection of ADM mAb resulted in significant suppression of CNV formation (Fig. 4D).

Discussion

In the current study, we have explored the possibility that ADM exerts angiogenic effects in a laser-induced CNV model. The ADM receptor was expressed in choroidal endothelial cells and ADM was upregulated in the choroid/RPE complex during CNV formation. Moreover, an ADM pharmaceutical antagonist and a mAb to ADM efficiently suppressed CNV formation and mediated synergistic effects together with a potent VEGF-A inhibitor. These findings suggest that ADM could represent a therapeutic target and be an attractive option for the treatment of CNV in AMD.

The biological functions of ADM are well- recognized to be dilatation of resistance vessels [29,30], increases of cardiac output [31], regulation of vascular permeability [32] and contribution to mobilization, adhesion and differentiation into endothelial progenitor cells of bone marrow-derived cells [33,34,35]. Additionally, several lines of evidence have suggested that inhibiting the ADM pathway with antibodies or antagonists directed against ADM or ADM receptors can reduce angiogenesis and tumor cell proliferation in mouse cancer models [8]. Although ADM is reported to affect not only angiogenesis but also tumor cell proliferation via its autocrine and paracrine mechanisms in cancer, there is little data showing the involvement of ADM in a disease model whose central pathogenesis depends on sprouting angiogenesis [11,12,13,16,23].

ADM immunoreactivity was reported in cardiac myocytes, vascular smooth muscle cells, ECs, renal distal and collecting tubules, mucosal and glandular epithelia of the digestive, respiratory and reproductive system, the endocrine and neuroendocrine system, as well as in the central nervous system [29]. In the current model, upregulation of ADM was not detected in the retina after laser treatment (data not shown), although Blom et al. reported the expression of ADM in neural retina. However, we saw ADM in the RPE/choroid. Secreted inflammatory cytokines after laser burn might be enhancing ADM expression and further accumulation of inflammatory cells.

This was confirmed using a primary RPE/choroid culture model in the present study. However, ADM expression 24 hr after TNF-α stimulation was lower than at 12 hr, in contrast to findings

with different cell lines such as RAW 264.7, RPE-19 and bEnd.3. We hypothesize that this difference can be attributed to the use of transformed cell lines which could display different expression patterns compared to that of primary cultures. Local upregulation of ADM at each photocoagulated site could induce direct ADM effects, i.e. EC proliferation, migration and tube formation. Currently, anti-VEGF therapy has become the major treatment modality for neovascular AMD. However, numerous injections of the anti-VEGF drug may be required to maintain clinical benefit. Moreover, after treatment with anti-VEGF drugs, it can be hypothesized that a hypoxic response could occur and subsequently upregulate ADM, because this has been observed in ECs [25] [36]. Chen et al. reported reciprocal regulation of ADM and HIF-1α expression exerted synergistic effects on proliferation of ECs in vitro [36]. Induction and nuclear translocation of HIF-1 α controls the expression of several angiogenic factors [37]. Therefore, the requirement for additional drugs together with anti-VEGF therapy is rational even if anti-ADM treatment partially suppresses CNV formation.

Although we expected that ADM injection would enhance the angiogenic response, exogenous ADM did not alter the size of CNV. We hypothesize that ADM was already saturated in the lesion and therefore additional factor would not be able to further activate the ADM receptor and exert any greater effects.

Chen et al. reported that tumor-associated macrophages (TAM) express both ADM and ADM receptor components. They also reported that ADM from TAM stimulated ECs and furthered angiogenesis via a paracrine pathway; moreover, it also potentiated the differentiation of TAM from the M1 to M2 state in an autocrine manner [23]. In the current study, infiltrating macrophages in CNV eyes expressed more ADM; therefore we cannot completely exclude the possibility that upregulation of ADM in macrophages could cause them to change their characteristics and to secrete other angiogenic factors such as VEGF. However, the finding of an inhibitory effect on EC proliferation of ADM antagonists in supernatant from macrophage cultures implies that ADM originating from macrophages must be at least partly responsible for CNV formation.

Udono et al. reported that hypoxia and inflammatory cytokines induced the expression of ADM in human RPE cells and that ADM could enhance RPE proliferation [26,38]. Therefore, in this CNV model, it is also possible that ADM expression in RPE was upregulated and that ADM secreted by RPE could promote angiogenesis. However, Huang et al. reported that ADM inhibited the migration of RPE cells in association with reductions in $[Ca^{2+}]$ [39]. Although there is some controversy about the function of ADM in RPE cells, we could demonstrate that inflammatory stimulation up-regulated the expression of ADM in RPE in vitro. Indeed, it is technically difficult to sort the RPE cells by flow cytometry using specific surface markers and we were unable to determine their ADM expression level. Although we have to carefully evaluate the major source of ADM in the CNV model, the observed paracrine and autocrine effects of ADM could induce CNV.

Supporting Information

Figure S1 Toxicity experiment of ADM (22–52) using bEnd.3. proliferation assay. ADM (22–52) could inhibit the proliferation of EC at 10 nM but there was no clear toxicity even at concentration of 100 μM. (*P<0.05).
(TIF)

Acknowledgments

We thank Keisho Fukuhara and Noriko Fujimoto for general assistance.

Author Contributions

Conceived and designed the experiments: SS MK KN NT. Performed the experiments: SS HK HN TW HS. Analyzed the data: SS HK NT DY. Contributed reagents/materials/analysis tools: SS MK KN NT. Wrote the paper: SS NT.

References

1. Dewan A, Liu M, Hartman S, Zhang SS, Liu DT, et al. (2006) HTRA1 promoter polymorphism in wet age-related macular degeneration. Science 314: 989–992.
2. Sakurai E, Anand A, Ambati BK, van Rooijen N, Ambati J (2003) Macrophage depletion inhibits experimental choroidal neovascularization. Invest Ophthalmol Vis Sci 44: 3578–3585.
3. Tsutsumi-Miyahara C, Sonoda KH, Egashira K, Ishibashi M, Qiao H, et al. (2004) The relative contributions of each subset of ocular infiltrated cells in experimental choroidal neovascularisation. Br J Ophthalmol 88: 1217–1222.
4. Xie P, Kamei M, Suzuki M, Matsumura N, Nishida K, et al. (2011) Suppression and regression of choroidal neovascularization in mice by a novel CCR2 antagonist, INCB3344. PLoS One 6: e28933.
5. Xiong M, Elson G, Legarda D, Leibovich SJ (1998) Production of vascular endothelial growth factor by murine macrophages: regulation by hypoxia, lactate, and the inducible nitric oxide synthase pathway. Am J Pathol 153: 587–598.
6. Poyner DR, Sexton PM, Marshall I, Smith DM, Quirion R, et al. (2002) International Union of Pharmacology. XXXII. The mammalian calcitonin gene-related peptides, adrenomedullin, amylin, and calcitonin receptors. Pharmacol Rev 54: 233–246.
7. McLatchie LM, Fraser NJ, Main MJ, Wise A, Brown J, et al. (1998) RAMPs regulate the transport and ligand specificity of the calcitonin-receptor-like receptor. Nature 393: 333–339.
8. Nikitenko LL, Fox SB, Kehoe S, Rees MC, Bicknell R (2006) Adrenomedullin and tumour angiogenesis. Br J Cancer 94: 1–7.
9. Iimuro S, Shindo T, Moriyama N, Amaki T, Niu P, et al. (2004) Angiogenic effects of adrenomedullin in ischemia and tumor growth. Circ Res 95: 415–423.
10. Shindo T, Kurihara Y, Nishimatsu H, Moriyama N, Kakoki M, et al. (2001) Vascular abnormalities and elevated blood pressure in mice lacking adrenomedullin gene. Circulation 104: 1964–1971.
11. Ishikawa T, Chen J, Wang J, Okada F, Sugiyama T, et al. (2003) Adrenomedullin antagonist suppresses in vivo growth of human pancreatic cancer cells in SCID mice by suppressing angiogenesis. Oncogene 22: 1238–1242.
12. Kaafarani I, Fernandez-Sauze S, Berenguer C, Chinot O, Delfino C, et al. (2009) Targeting adrenomedullin receptors with systemic delivery of neutralizing antibodies inhibits tumor angiogenesis and suppresses growth of human tumor xenografts in mice. FASEB J 23: 3424–3435.
13. Ouafik L, Sauze S, Boudouresque F, Chinot O, Delfino C, et al. (2002) Neutralization of adrenomedullin inhibits the growth of human glioblastoma cell lines in vitro and suppresses tumor xenograft growth in vivo. Am J Pathol 160: 1279–1292.
14. Kim W, Moon SO, Sung MJ, Kim SH, Lee S, et al. (2003) Angiogenic role of adrenomedullin through activation of Akt, mitogen-activated protein kinase, and focal adhesion kinase in endothelial cells. FASEB J 17: 1937–1939.
15. Ribatti D, Nico B, Spinazzi R, Vacca A, Nussdorfer GG (2005) The role of adrenomedullin in angiogenesis. Peptides 26: 1670–1675.
16. Hague S, Zhang L, Oehler MK, Manek S, MacKenzie IZ, et al. (2000) Expression of the hypoxically regulated angiogenic factor adrenomedullin correlates with uterine leiomyoma vascular density. Clin Cancer Res 6: 2808–2814.
17. Gavard J, Hou X, Qu Y, Masedunskas A, Martin D, et al. (2009) A role for a CXCR2/phosphatidylinositol 3-kinase gamma signaling axis in acute and chronic vascular permeability. Mol Cell Biol 29: 2469–2480.
18. Campa C, Kasman I, Ye W, Lee WP, Fuh G, et al. (2008) Effects of an anti-VEGF-A monoclonal antibody on laser-induced choroidal neovascularization in mice: optimizing methods to quantify vascular changes. Invest Ophthalmol Vis Sci 49: 1178–1183.
19. Naito H, Kidoya H, Sakimoto S, Wakabayashi T, Takakura N (2011) Identification and characterization of a resident vascular stem/progenitor cell population in preexisting blood vessels. EMBO J 31: 842–855.
20. Takakura N, Watanabe T, Suenobu S, Yamada Y, Noda T, et al. (2000) A role for hematopoietic stem cells in promoting angiogenesis. Cell 102: 199–209.

21. Sakimoto S, Kidoya H, Naito H, Kamei M, Sakaguchi H, et al. (2012) A role for endothelial cells in promoting the maturation of astrocytes through the apelin/APJ system in mice. Development 139: 1327–1335.
22. Grossniklaus HE, Kang SJ, Berglin L (2010) Animal models of choroidal and retinal neovascularization. Prog Retin Eye Res 29: 500–519.
23. Chen P, Huang Y, Bong R, Ding Y, Song N, et al. (2011) Tumor-associated macrophages promote angiogenesis and melanoma growth via adrenomedullin in a paracrine and autocrine manner. Clin Cancer Res 17: 7230–7239.
24. Kubo A, Minamino N, Isumi Y, Katafuchi T, Kangawa K, et al. (1998) Production of adrenomedullin in macrophage cell line and peritoneal macrophage. J Biol Chem 273: 16730–16738.
25. Ogita T, Hashimoto E, Yamasaki M, Nakaoka T, Matsuoka R, et al. (2001) Hypoxic induction of adrenomedullin in cultured human umbilical vein endothelial cells. J Hypertens 19: 603–608.
26. Udono T, Takahashi K, Nakayama M, Murakami O, Durlu YK, et al. (2000) Adrenomedullin in cultured human retinal pigment epithelial cells. Invest Ophthalmol Vis Sci 41: 1962–1970.
27. Saita M, Shimokawa A, Kunitake T, Kato K, Hanamori T, et al. (1998) Central actions of adrenomedullin on cardiovascular parameters and sympathetic outflow in conscious rats. Am J Physiol 274: R979–984.
28. Boguslawski G, McGlynn PW, Harvey KA, Kovala AT (2004) SU1498, an inhibitor of vascular endothelial growth factor receptor 2, causes accumulation of phosphorylated ERK kinases and inhibits their activity in vivo and in vitro. J Biol Chem 279: 5716–5724.
29. Eto T (2001) A review of the biological properties and clinical implications of adrenomedullin and proadrenomedullin N-terminal 20 peptide (PAMP), hypotensive and vasodilating peptides. Peptides 22: 1693–1711.
30. Ishiyama Y, Kitamura K, Ichiki Y, Nakamura S, Kida O, et al. (1993) Hemodynamic effects of a novel hypotensive peptide, human adrenomedullin, in rats. Eur J Pharmacol 241: 271–273.
31. Rademaker MT, Charles CJ, Lewis LK, Yandle TG, Cooper GJ, et al. (1997) Beneficial hemodynamic and renal effects of adrenomedullin in an ovine model of heart failure. Circulation 96: 1983–1990.
32. Hippenstiel S, Witzenrath M, Schmeck B, Hocke A, Krisp M, et al. (2002) Adrenomedullin reduces endothelial hyperpermeability. Circ Res 91: 618–625.
33. Abe M, Sata M, Suzuki E, Takeda R, Takahashi M, et al. (2006) Effects of adrenomedullin on acute ischaemia-induced collateral development and mobilization of bone-marrow-derived cells. Clin Sci (Lond) 111: 381–387.
34. Iwase T, Nagaya N, Fujii T, Itoh T, Ishibashi-Ueda H, et al. (2005) Adrenomedullin enhances angiogenic potency of bone marrow transplantation in a rat model of hindlimb ischemia. Circulation 111: 356–362.
35. Kong XQ, Wang LX, Yang CS, Chen SF, Xue YZ, et al. (2008) Effects of adrenomedullin on the cell numbers and apoptosis of endothelial progenitor cells. Clin Invest Med 31: E117–122.
36. Chen L, Qiu JH, Zhang LL, Luo XD (2012) Adrenomedullin promotes human endothelial cell proliferation via HIF-1alpha. Mol Cell Biochem 365: 263–273.
37. Pugh CW, Ratcliffe PJ (2003) Regulation of angiogenesis by hypoxia: role of the HIF system. Nat Med 9: 677–684.
38. Udono T, Takahashi K, Nakayama M, Yoshinoya A, Totsune K, et al. (2001) Induction of adrenomedullin by hypoxia in cultured retinal pigment epithelial cells. Invest Ophthalmol Vis Sci 42: 1080–1086.
39. Huang W, Wang L, Yuan M, Ma J, Hui Y (2004) Adrenomedullin affects two signal transduction pathways and the migration in retinal pigment epithelial cells. Invest Ophthalmol Vis Sci 45: 1507–1513.

THE JOURNAL OF BIOLOGICAL CHEMISTRY VOL. 288, NO. 18, pp. 12469–12477, May 3, 2013

Ligand-independent Tie2 Dimers Mediate Kinase Activity Stimulated by High Dose Angiopoietin-1*[S]

Received for publication, November 5, 2012, and in revised form, February 19, 2013 Published, JBC Papers in Press, March 15, 2013, DOI 10.1074/jbc.M112.433979

Daishi Yamakawa[‡], Hiroyasu Kidoya[‡], Susumu Sakimoto[‡], Weizhen Jia[‡], Hisamichi Naito[‡], and Nobuyuki Takakura[‡§1]

From the [‡]Department of Signal Transduction, Research Institute for Microbial Diseases, Osaka University, 3-1 Yamada-oka, Suita-shi, Osaka 565-0871, Japan and [§]Japan Science and Technology Agency (JST), Sanbancho, Chiyoda-ku, Tokyo 102-0075, Japan

Background: Tie2 is essential for angiogenesis and vascular stabilization.
Results: Tie2, but not Tie1, forms ligand-independent dimers on the cell surface.
Conclusion: The inactive monomer mutant Tie2YIA/LAS decreases Ang1/Tie2 signaling.
Significance: The Tie2 ligand-independent dimer induces strong phosphorylation upon high dose Ang1 binding.

Tie2 is a receptor tyrosine kinase expressed on vascular endothelial cells (ECs). It has dual roles in promoting angiogenesis and stabilizing blood vessels, and it has been suggested that Tie2 forms dimers and/or oligomers in the absence of angiopoietin-1 (Ang1); however, the mechanism of ligand-independent dimerization of Tie2 and its biological significance have not been clarified. Using a bimolecular fluorescence complementation assay and a kinase-inactive Tie2 mutant, we show here that ligand-independent Tie2 dimerization is induced without Tie2 phosphorylation. Moreover, based on the fact that Tie1 never forms heterodimers with Tie2 in the absence of Ang1 despite having high amino acid sequence homology with Tie2, we searched for ligand-independent dimerization domains of Tie2 by reference to the difference with Tie1. We found that the YIA sequence of the intracellular domain of Tie2 corresponding to the LAS sequence in Tie1 is essential for this dimerization. When the YIA sequence was replaced by LAS in Tie2 (Tie2YIA/LAS), ligand-independent dimer was not formed in the absence of Ang1. When activation of Tie2YIA/LAS was induced by a high dose of Ang1, phosphorylation of Tie2 was limited compared with wild-type Tie2, resulting in retardation of activation of Erk downstream of Tie2. Therefore, these data suggest that ligand-independent dimerization of Tie2 is essential for a strong response upon stimulation with high dose Ang1.

The functions of angiopoietin-1 (Ang1),[2] a ligand for receptor tyrosine kinase Tie2 expressed on endothelial cells (ECs), in both EC-to-EC and EC-to-mural cell adhesion are well established (1–4). Although Ang1-Tie2 signaling is involved in promoting maturation and quiescence of blood vessels mainly regulated by Akt signal transduction via the p85 subunit of PI3K, Tie2 also has proangiogenic activity mediated by MAPK signaling (5–7). Because Tie2 possesses both anti-angiogenic as well as proangiogenic properties, it is important to investigate how Tie2 activation is altered during angiogenesis. The Tie receptor family consists of Tie2 and Tie1 (8–10). Recent studies show that Ang1 activates Tie1 indirectly by interactions with Tie2 (11). When Tie1 expression is silenced, Tie2 signaling especially via the MAPK pathway is enhanced; accordingly, Tie1-deficient mice show hyperproliferative vascular formation and vascular abnormalities (12, 13). This suggests that Tie1 may negatively regulate angiogenic signaling by Tie2.

Tie2 is composed of an extracellular domain, one transmembrane domain, and an intracellular tyrosine kinase domain split into two by a non-kinase sequence. Tie1 has high amino acid sequence homology with Tie2 (76 and 33% identity in intracellular and extracellular domains, respectively). Based on the isolation of Tie2 ligands and analysis of signal transduction through Tie2, it is widely accepted that Ang1 activates Tie2, but Ang2 binding inhibits its signaling. Thus, with certain exceptions Ang2 acts as an Ang1 antagonist (4, 13–18).

It is known that Tie2 is present on the EC surface in the form of dimers and higher order oligomers, as established by electron microscopy (19). It has been reported that EGF receptor, erythropoietin receptor, and TNF receptor also dimerize in a ligand-independent manner (20–25). Ligand-independent dimerization of EGF receptor does not lead to tyrosine phosphorylation of EGF receptor. It has been suggested that a conformational change of the EGF receptor induces kinase activity on ligand binding. Therefore, ligand-independent dimers may mediate rapid signal transduction responses. Although Tie2 also forms ligand-independent dimers, the importance of this has not yet been determined.

In the present study, we established a system for visualization of Tie2 dimers using bimolecular fluorescence complementation (BiFC) assays in living cells (26). Using this system, we sought Ang1-independent Tie2-Tie2 dimerization domains. We generated a Tie2 mutant that does not form dimers in the absence of Ang1. We investigated the biological significance of ligand-independent Tie2 dimerization using this mutant.

* This work was supported in part by a grant from the Ministry of Education, Science, Sports, and Culture of Japan.
[S] This article contains supplemental Table S1 and Figs. S1–S6.
[1] To whom correspondence should be addressed: Dept. of Signal Transduction, Research Institute for Microbial Diseases, Osaka University, 3-1 Yamada-oka, Suita-shi, Osaka 565-0871, Japan. Tel.: 81-6879-8316; Fax: 81-6879-8314; E-mail: ntakaku@biken.osaka-u.ac.jp.
[2] The abbreviations used are: Ang1, angiopoietin-1; EC, endothelial cell; BiFC, bimolecular fluorescence complementation; Ab, antibody.